

**DOKUZ EYLÜL UNIVERSITY**  
**GRADUATE SCHOOL OF NATURAL AND APPLIED SCIENCES**

**ELECTRONIC STRUCTURE OF THE QUANTUM WIRES**  
**WITH SPIN-ORBIT INTERACTIONS**  
**UNDER THE INFLUENCE OF**  
**IN-PLANE MAGNETIC FIELDS**

by

**Bircan GİŞİ**

**July, 2012**

**İZMİR**

**ELECTRONIC STRUCTURE OF THE QUANTUM WIRES  
WITH SPIN-ORBIT INTERACTIONS  
UNDER THE INFLUENCE OF  
IN-PLANE MAGNETIC FIELDS**

**A Thesis Submitted to the  
Graduate School of Natural and Applied Sciences of Dokuz Eylül University  
In Partial Fulfillment of the Requirements for the Degree  
of Master of Science in  
Physics**

**by**

**Bircan GİŞİ**

**July, 2012  
İZMİR**

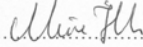
M.Sc. THESIS EXAMINATION RESULT FORM

We have read the thesis entitled "ELECTRONIC STRUCTURE OF THE QUANTUM WIRES WITH SPIN-ORBIT INTERACTIONS UNDER THE INFLUENCE OF IN-PLANE MAGNETIC FIELDS" completed by BİRCAN GİŞİ under supervision of ASSIS. PROF. DR. SERPİL ŞAKİROĞLU and we certify that in our opinion it is fully adequate, in scope and in quality, as a thesis for the degree of Master of Science.

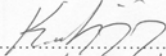


.....  
Assis. Prof. Dr. Serpil ŞAKİROĞLU

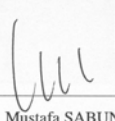
Supervisor



.....  
Yard. Doç. Dr. F. Mine GAPAR  
(Jury Member)



.....  
Yard. Doç. Dr. Kerem Akdoğan  
(Jury Member)



.....  
Prof. Dr. Mustafa SABUNCU  
Director

Graduate School of Natural and Applied Sciences

## ACKNOWLEDGEMENTS

The work would not have been possible without the guidance and the help of several individuals who in one way or another contributed and extended their valuable assistance in the preparation and completion of this thesis.

Firstly, I wish to express my utmost gratitude to my supervisor Assis. Prof. Dr. Serpil ŞAKİROĞLU, for her excellent guidance, endless patience during this research as well as giving me extraordinary experiences throughout the work. Above all and the most needed, she provided me unflinching encouragement and support in various ways. She exceptionally inspired and enriched my growth as a student, as a researcher and a scientist want to be. I am indebted to her more than she knows.

I gratefully acknowledge Prof. Dr. İsmail SÖKMEN for much support, excellent motivation, fruitful discussions, valuable recommendations and crucial contribution which made him a backbone of this research and so to this thesis. He shared his thorough knowledge and expertise in semiconductor and computational physics. He taught me not only being responsible and disciplined but also being cheerful always.

My thanks to go in particular to Assis. Prof. Dr. Kadir AKGÜNGÖR for his valuable advice in science discussions, recommendations and contributions.

I gratefully thank to my friends Yenil, Kübra, Sevil, Dilek, Mehmet, Aslı and Zeynep. The days would have passed far more slowly without the support of my friends who shared their humor and encouraged me on this journey.

I would like to express my thanks to The Scientific and Technological Research Council of Turkey (TÜBİTAK BİDEB 2210) for supporting me during my thesis.

My special thanks to my peerless family. Without their love, continual encouragement and endless support this work would not have been possible. Sevcan, Canan, Çağla thank you for being my sister and thanks to Nihat for being as my brother. And I have no words to thank to my parents Sabiha and Nurettin for their unconditional love and support through out my life.

Bircan GİŞİ

*ailleme ...*

# ELECTRONIC STRUCTURE OF THE QUANTUM WIRES WITH SPIN-ORBIT INTERACTIONS UNDER THE INFLUENCE OF IN-PLANE MAGNETIC FIELDS

## ABSTRACT

In this thesis, we have made a theoretical investigation of electronic ground state structure of a parabolically confined quantum wire subjected to an in-plane magnetic field, including spin-orbit interactions and exchange-correlation effects. In this study, the effect of generally off-neglected cubic Dresselhaus spin-orbit interaction has also been taken into account. The energy dispersion has been numerically calculated in a wide range of linear electron densities. The effects of the exchange-correlation interaction have been investigated within the noncollinear local-spin density approximation. A self-consistent solution of the Kohn-Sham equations has been implemented. The energy eigenvalues and the eigenfunctions of the system have been obtained from numerical solutions of Schrödinger equation. One-dimensional finite elements method based on Galerkin procedure has been used.

It has been seen that the structure of energy subband depends strongly on the strength of spin-orbit interaction, the magnitude and the orientation angle of magnetic field and the exchange-correlation effects. It has been shown that in the presence of an external magnetic field the interplay of different types of spin-orbit interaction and Zeeman effect leads to complicated and intriguing energy dispersion for different spin branches. Including exchange-correlation energy has been caused anomalous plateaus which could play an important role for understanding of the conductance. We have seen that our results are compatible with the studies in the litterateur. We have found different results for exchange-correlation effect especially in low density limits that could be due to the use of different parametrization for exchange-correlation energy functional.

**Keywords:** Quantum wire, spin-orbit interaction, exchange-correlation energy.

# DÜZLEM MAGNETİK ALAN ALTINDA SPIN-YÖRÜNGE ETKİLEŞİMLİ KUANTUM TELLERİNİN ELEKTRONİK YAPISI

## ÖZ

Bu tezde, düzlem manyetik alan altındaki parabolik hapsedilmiş kuantum telinin elektronik taban durumu yapısını, spin-yörünge etkileşimleri ve deęiřtokuř-korelasyon etkilerini içerecek řekilde, teorik olarak inceledik. Bu çalıřmada, genellikle ihmal edilen kübik Dresselhaus spin-yörünge etkileřme etkisi de hesaba katıldı. Enerji daęınımı lineer elektron yoğunluęunun geniř bir aralıęında nümerik olarak hesaplandı. Deęiřtokuř-korelasyon etkileřim etkileri eřçizgisel olmayan yerel-spin yoğunluk yaklařımı dahilinde incelendi. Kohn-Sham denklemlerinin özuyumlu çözümleri gerçekteřirildi. Sistemin enerji özdeęerleri ve özfonksiyonları Schrödinger denkleminin sayısal çözümlerinden elde edildi. Galerkin yöntemine dayalı olan bir-boyutta sonlu elemanlar yöntemi kullanıldı.

Enerji altbant yapısının spin-yörünge etkileřimine, manyetik alanın büyüklüęüne ve yönelim açısına ve deęiřtokuř-korelasyon etkisine güçlü bir řekilde baęlı olduęu görüldü. Dıř manyetik alan varlıęında farklı tipteki spin-yörünge etkileřimi ile Zeeman etkisinin etkileřiminin farklı spin dalları için karmařık ve řařırtıcı enerji daęınımına yol açtıęı gösterildi. Deęiřtokuř-korelasyon enerjisinin eklenmesi iletkenlięin anlaşılmasında önemli rol oynayabilecek olan olaęandıřı platoların oluşmasına sebep oldu. Sonuçlarımızın literatürdeki çalıřmalarla uyumlu olduęunu gördük. Özellikle düşük yoğunluk limitinde deęiřtokuř-korelasyon etkileri için farklı sonuçlar elde ettik bu farklı deęiřtokuř-korelasyon enerji fonksiyoneli kullanılmasından kaynaklanabilir.

**Anahtar sözcükler:** Kuantum teli, spin-yörünge etkileřimi, deęiřtokuř-korelasyon enerjisi.

# CONTENTS

	<b>Page</b>
ACKNOWLEDGEMENTS .....	iii
ABSTRACT .....	v
ÖZ.....	vi
<b>CHAPTER ONE - INTRODUCTION .....</b>	<b>1</b>
<b>CHAPTER TWO - QUANTUM WIRES .....</b>	<b>3</b>
<b>CHAPTER THREE-SPIN-ORBIT INTERACTION .....</b>	<b>7</b>
3.1 From Dirac Equation to Spin-Orbit Coupling .....	7
3.2 Semiconductor Spintronics .....	9
3.3 Spin-Orbit Interaction.....	9
3.3.1 Rashba Spin-Orbit Interaction .....	10
3.3.2 Dresselhaus Spin-Orbit Interaction .....	10
3.4 Zeeman Effect .....	11
<b>CHAPTER FOUR - THEORETICAL BACKGROUND .....</b>	<b>12</b>
4.1 Schrödinger Equation .....	12
4.2 Fundamental Approximations to Schrödinger Equation .....	12
4.2.1 Born-Oppenheimer Approximation .....	12
4.2.2 Hartree Approximation .....	13
4.2.3 Hartree-Fock Approximation .....	14
4.3 Density Functional Theory .....	15
4.3.1 Hohenberg-Kohn Theorems .....	17
4.3.2 Kohn-Sham Equations .....	18
4.4 Exchange-Correlation Energy .....	21
4.4.1 Local Density Approximation .....	22
4.4.2 The Local Spin Density Approximation .....	22
4.5 Theoretical Methods .....	23
4.5.1 Variational Principle .....	23
4.5.2 Finite Element Method.....	24



<b>CHAPTER FIVE - FORMALISM</b> .....	<b>33</b>
5.1 System and Its Variables .....	33
5.2 Kohn-Sham Hamiltonian .....	36
5.3 Noncollinear Local-Spin Density Approximation .....	41
<b>CHAPTER SIX - RESULTS</b> .....	<b>45</b>
6.1 The Effect of Spin-Orbit Interaction and Magnetic Field .....	46
6.2 The Effects of Exchange-Correlation Energy .....	52
<b>CHAPTER SEVEN - CONCLUSION</b> .....	<b>59</b>
<b>REFERENCES</b> .....	<b>61</b>

## **CHAPTER ONE**

### **INTRODUCTION**

In the past 40 years, semiconductor physics brought a revolution, both in science and in everyday life technology. The advent of semiconducting devices and their use in integrated circuits was a social revolution and clearly marked the brink of a new era. With the development of this new technology, the tendency to produce high precision nanostructured electronic devices has been increased. Producing these devices has prompted intense activity in the study of semiconductor heterostructures. These new devices exploit electron spin rather than electron charge and due to their low dimensional features they are faster and more powerful than those existing. Spintronics is a new emerging field based on the electron spin and promises possible applications in many fields such as electronics, quantum information etc. The main goal of spintronics is carrying out controllable manipulations of electron spins using intrinsic spin-orbit (SO) interactions. These SO interactions occur in the existence of macroscopic electric fields which arise from inversion asymmetry properties characteristic of the heterostructures. Two basic mechanisms of the spin-orbit interaction are Rashba and Dresselhaus coupling (Zhang, Zhao, & Liu, 2009). The inversion asymmetry of the confining potential in the growth direction induces Rashba SO coupling and the bulk inversion asymmetry of the heterostructure causes Dresselhaus SO coupling.

Among semiconductor nanostructures, quantum wires (QW)s are especially well-suited for the development of spintronic devices. Their transverse length can be externally controlled hence the system can be made more or less quasi-one-dimensional. In addition, the ratio of the SO strength to the confinement can also be adjusted. On the other hand, the electron motion can be rendered almost collisionless because of the high purity of two-dimensional electron gas (Malet, Marti, Barranco, Serra, & Lipparini, 2007).

The aim of this work is to make a theoretical investigation of the electronic structure of a parabolically confined QW subjected to an in-plane magnetic field, including both Rashba and Dresselhaus SO interactions and exchange-correlation effects. We choose the wire plane to be  $xy$ -plane with  $y$ -direction parallel to wire. We have inves-

tigated energy dispersion in a wide range of linear electronic densities in the presence of strong and weak SO coupling that are characterized according to value of ratio of SO coupling to confining energy. We take into account the generally off-neglected cubic Dresselhaus SO interactions. The effects of the exchange-correlation interaction on the energy subband structure of QW has been investigated within the noncollinear local-spin density approximation in the framework of density functional theory. The exchange-correlation potential was defined by using the energy functional of Attaccalite and coworkers (Attaccalite, Moroni, Gori-Giorgi, & Bachalet, 2002; Attaccalite, Moroni, Gori-Giorgi, & Bachalet, 2003). We implemented a self-consistent solution of the Kohn-Sham equations for a QW submitted to a parabolic lateral confinement.

This work is organized as follows: In Chapter 2 we give a brief overview of quantum wires and their fabrication techniques. We present the spin-orbit interaction and Zeeman effect in Chapter 3. Chapter 4 is devoted to introduce the theory and formalism used in this work. The definition of the system and its properties are given in Chapter 5. In Chapter 6 we give the numerical results of quantum wires in different conditions such as different strength of SO interaction, magnetic field and exchange-correlation energy. A short concluding chapter summarizes our findings.

## CHAPTER TWO

### QUANTUM WIRES

Technology and science has opened a new era via the bulk crystalline semiconductor. With the electronic and optical features they constitute the basis of industry such as electronics, spintronics, telecommunications, microprocessors, computers and many other components of modern technology. A typical example for bulk crystalline is semiconductor heterostructure which is formed by combination of two or more heterojunctions together in a device (Wagner, 2009). A heterojunction is composed of more than one material which has same lattice constant but different band gaps.

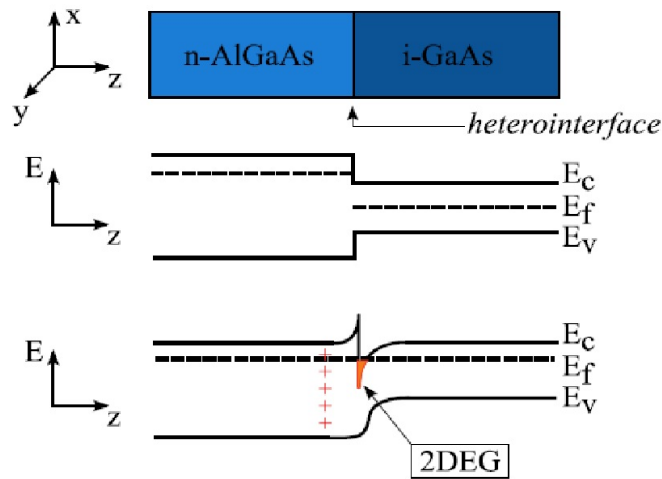


Figure 2.1 A 2-dimensional electron gas is formed at the interface between intrinsic GaAs and n-doped AlGaAs.

A well known example is  $GaAs/Al_xGa_{1-x}As$  alloy which consist of semiconductor gallium (Ga), arsenide (As) and aluminium (Al), thus forming a heterointerface (Harrison, 2005). The lattice constant is same for two alloys but it is clearly seen that the band gaps are different and the edges of conduction and valance bands are not in the align. When these two crystals bring together, electrons start to spill over from n-AlGaAs leaving behind positively charged donors. The electrostatic potential bends the bands as seen in Figure 2.1. When the system achieve the equilibrium, the Fermi energy is constant everywhere. The conduction band at the interface constitutes a triangular

quantum well crossing the Fermi energy and a very thin layer occurs. The electrons are restricted only perpendicular to the interface, thus a two-dimensional electron gas is obtained.

The two-dimensional electron gas can be confined by application of gate voltages. The motion of at least one type of charge carriers is confined in at least one direction which spatial dimension can be compared to the de-Broglie wavelength of charge carriers. Therefore the semiconductor can be called to be of reduced dimensionality. Reduction in dimensionality can be developed by reducing the dimensionality of the electron's environment from a two-dimensional quantum well to a one-dimensional quantum wire and to a zero-dimensional quantum dot.

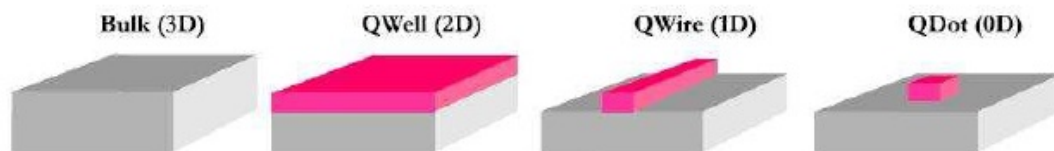


Figure 2.2 Schematic representation of the quantum well, wire and dot.

In the quantum wells, the electrons are localized in the direction perpendicular to the layer and they can move freely in the layer plane. The electrons are localized in two directions in the QWs and their motion has freedom along the wire axis. The quantum dots are confined in all three directions as a result they have discrete energy spectrum.

QWs have been studied intensively worldwide both theoretically and experimentally ( Canham, 1990; Quay et al, 2010; Gujarathi, Alam, & Pramanik, 2012). The one-dimensional structures such as QWs take interest in for fundamental research because of their unique structural and physical properties which arise from their characteristic bulk structure. On the other hand they promise fascinating potential for future technology such as microelectronic and opto-electronic devices (Alferov, 2001). These structures have been studied extensively in order to investigate their electronic, spin, transport and conductance properties (Orellana, Dominguez-Adame, Gomez, & de Guevera, 2003; Abonov, Pokrovsky, Saslow, & Zhou, 2012).

QWs can be produced by some fabrication techniques such as molecular-beam epitaxy (Gonzalez et al, 2000; Garcia, Gonzales, Silveria, Gonzales, Y., & Brianes, 2001), electron-beam lithography, wet/dry chemical etching (Petroff, Gassard, Logan, & Wiegmann, 1982), and epitaxial growth techniques which can be separated as V-shaped (Kapon, Hwang, & Bhat, 1989) and T-shaped (Pfeiffer et al, 1990). The quantum wire can be also obtained by confining the electrons in two-dimensions. de Picciotto and his coworkers (de Picciotto, Stormer, Pfeiffer, Baldwin, & West, 2001) fabricate quantum wires by cleaved-edge overgrowth on GaAs/AlGaAs heterostructures as shown Figure 2.3. Three tungsten gate electrodes on the surface of the device define two strips of two-dimensional electron gas that serve as voltage probes for the central part of the wire. As the width of these strips is small compared with the scattering length in the wire, the perturbation caused by the voltage probes is negligible.

After mentioning about the fabrication process of quantum wires, it may be useful to briefly summarize the numerical calculating techniques. A serious effort was spent to develop their theoretical modelling in order to predict the physical properties of such structures and to understand experimental results. The energy band structure forms the basis of understanding the most optical properties of semiconductors. Their confinement leads to a discrete energy spectrum, namely electrons and holes occupy discrete quantum levels. The energy band diagrams and the wave functions of quantum wires are very complicated to calculate. Generally the analytic solution is not possible except some circumstances. For the analysis of quantum wires several numerical techniques have been developed, such as effective bond orbital method (Citrin, & Chang, 1989), tight binding method (Yamauchi, Takahasi, & Arakowa, 1991), finite difference method (Pryor, 1991), and finite-element method (FEM) (Searles, & Felsobuki, 1988; Kojimo, Mitsunaga, & Kyuma, 1989).

All of these methods base on basis functions and the number of the basis function determine the convenience of the method. On the other hand, FEM is more useful method due to the requirement only a few basis functions at each atomic site to describe the electronic band structure accurately, depending on whether the spin-orbit split-off bands are neglected or not. The advantage of FEM over a numerical technique is that it can analyze accurately energy eigenstates and wave functions of arbitrarily shaped

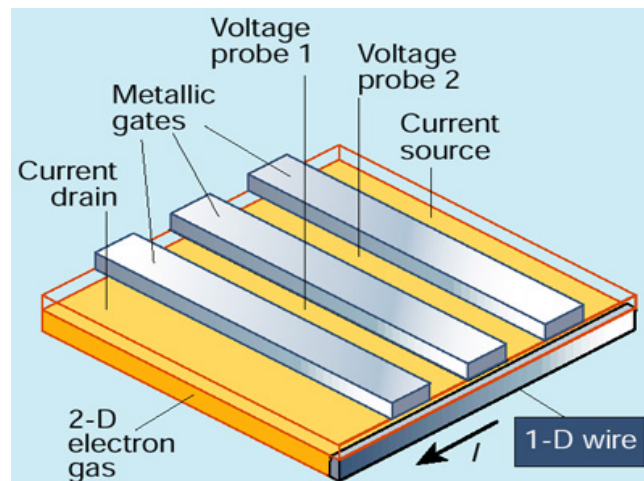


Figure 2.3 Fabrication of quantum wire (de Picciotto et al, 2001).

geometries with wide range of lateral dimensions. For an arbitrary shaped quantum wire the energy levels and the wave functions were calculated by Kojima (Kojima et al, 1989) and his co-workers. An investigation of valence band structures and optical properties of quantum wire was carried out by Yi and Dagli (Yi, & Dagli, 1995) via using a four band  $\mathbf{k} \cdot \mathbf{p}$  analysis by FEM. Using the FEM the valence band mixing effect, the strain effect, and the crystallographic orientation effect on the valence-subband structures of quantum wire was analyzed by Ogawa (Ogawa, Kunimasa, Ito, & Miyoshi, 1988). And in this thesis, the single particle states has been calculated with high accuracy by FEM.

## CHAPTER THREE

### SPIN-ORBIT INTERACTION

#### 3.1 From Dirac Equation to Spin-Orbit Coupling

SO interactions are important in transport and manipulation of electron spins in two-dimensional electron gas channels (Jalil, Tan, & Fujita, 2008). When a charge carrier travels in an electric field, in its restframe it sees a moving electric field. These moving charges, due to electric field, give rise to an internal magnetic field and this internal magnetic field couples to the spin of the electron (Meijer, 2005). The ability of couple the spin and charge conductance helps to approach investigation of electronics, photonics and spintronics in semiconductors. Quasi-two-dimensional semiconductor structures such as QWs and heterostructures are well suited for a systematic investigation of SO coupling effects (Wrinkler, 2003). Some of features especially spatial properties of electrons, moving through the periodic crystal, can be determined by energy bands  $E_{nk}$ .

SO interaction which is a relativistic effect can be obtained by taking the nonrelativistic limit of the Dirac equation. The derivation is based on Pauli equation and it has been taken Sakurai (Sakurai, 1967). The Hamiltonian form of the Dirac equation in the standart formalism can be written as  $H|\psi\rangle = E|\psi\rangle$ .

$$H = \begin{pmatrix} 0 & c\boldsymbol{\sigma}\cdot\mathbf{p} \\ c\boldsymbol{\sigma}\cdot\mathbf{p} & 0 \end{pmatrix} + \begin{pmatrix} mc^2 & 0 \\ 0 & -mc^2 \end{pmatrix} \quad (3.1.1)$$

where  $c$  is the speed of light,  $\mathbf{p}$  is the momentum and  $\boldsymbol{\sigma}$  are Pauli spin matrices. From  $|\psi\rangle = (\psi_A, \psi_B)^T$ , one can obtain two coupled equation for  $\psi_A$  and  $\psi_B$ . Eliminating  $\psi_B$

$$\mathbf{p}\cdot\boldsymbol{\sigma}\frac{c^2}{E+mc^2}\mathbf{p}\cdot\boldsymbol{\sigma}\psi_A = (E-mc^2)\psi_A \quad (3.1.2)$$

If a potential  $V$  exist in the system  $E-V$  can be written instead of  $E$ . The derivation is calculated in the nonrelativistic regime so  $E = mc^2 + \epsilon$  where  $\epsilon \ll mc^2$ .  $|V| \ll mc^2$  is assumed and this expansion is obtained



$$\frac{c^2}{E - V + mc^2} = \frac{1}{2m} \left( 1 - \frac{\varepsilon - V}{2mc^2} + \dots \right) \quad (3.1.3)$$

Using the  $(\mathbf{p} \cdot \boldsymbol{\sigma})(\mathbf{p} \cdot \boldsymbol{\sigma}) = p^2$  knowledge, simply Schrödinger equation emerges

$$\left( \frac{p^2}{2m} + V \right) \psi = \varepsilon \psi \quad (3.1.4)$$

The reason this derivation works is that to zeroth order in  $(v/c)$ ,  $\psi_B = 0$ . In fact, from Equation 3.1.1 we have to first order in  $(v/c)^2$

$$\psi_B = \frac{\mathbf{p} \cdot \boldsymbol{\sigma}}{2mc} \psi_A \quad (3.1.5)$$

Namely, in this frame  $\psi_A$  is equivalent to the Schrödinger wave function  $\psi$ . In accordance with Dirac theory the wave functions have to be normalized.

$$\int (\psi_A^\dagger \psi_A + \psi_B^\dagger \psi_B) = 1 \quad (3.1.6)$$

From Equation 3.1.5, writing  $\psi_A$  instead of  $\psi_B$

$$\int \psi_A^\dagger \left( 1 + \frac{p^2}{4mc^2} \right) \psi_A = 1 \quad (3.1.7)$$

To obtain normalize wave function,  $\psi = [1 + p^2/(8mc^2)]\psi_A$  should be taken. Equation 3.1.3 is substituted in Dirac equation and Pauli equation is obtained.

$$\left( \frac{p^2}{2m} + V - \frac{p^2}{8mc^2} - \frac{\hbar}{4mc^2} \boldsymbol{\sigma} \cdot \mathbf{p} \times \nabla V + \frac{\hbar^2}{8mc^2} \nabla^2 V \right) \psi = \varepsilon \psi \quad (3.1.8)$$

Every term in the equation can be addressed one by one. The third term is a relativistic correction to the kinetic energy, presented as a first term, and the last term gives the shift in the energy. And the fourth term is the SO coupling term in the general form the three-dimension SO interaction Hamiltonian.

$$\mathcal{H}_{SO} = -\frac{\hbar}{4m_0^2 c^2} \boldsymbol{\sigma} \cdot (\mathbf{p} \times \nabla V(\mathbf{r})) \quad (3.1.9)$$

where  $m_0$  is the mass of free electron,  $c$  the speed of light,  $\hbar$  Planck's constant  $\boldsymbol{\sigma}$

the vector of Pauli matrices and  $V(\mathbf{r})$  the electrical potential.  $V(\mathbf{r})$  is called Coulomb potential in atomic physics.

### 3.2 Semiconductor Spintronics

Electron spin rather than charge is the key property of semiconductor spintronics. Spin-dependent phenomena in semiconductor have a serious potential for development future spintronic devices so they have motivated an intense study field in recent years (Zutic, Fabian, & Sarma, 2004; Nitta, 2004; Choi, Kakegawa, Akabori, Suzuhi, & Yamada, 2008). In semiconductor spintronics the basic idea is combining semiconductor microelectronics with spin dependent effects for development of new devices. Spintronics emerges attractively in fabricating these new information storage devices. But there are some difficulties in production of semiconductor based spintronics devices. One of the major obstacle is producing the magnetic fields which control the electron spins. But effectively varying external magnetic fields over device length scales, which are measured in nanometers, is not considered feasible. To get rid of this problem there are two ways. One of them is to use dilute magnetic semiconductors (Dietl, 1994, 2010). The other way is to use electric fields to carry out controllable manipulations of electron spins through SO interactions (Wu, Jiang, & Weng, 2010).

### 3.3 Spin-Orbit Interaction

SO interactions have an effective impact on the energy subband structure and the interactions arise from some sources. In solid systems, electric field generally causes SO interactions in three different types. They can be written as impurities in the conduction band, lack of crystal inversion symmetry and lack of structural inversion asymmetry of the confinement potential of electrons in a heterostructure. The SO interaction which is induced by impurities can be neglected in practise because its effect is very weak in the presence of other two mechanism. If impurities is the only SO interaction source then it can't be neglected. Most of III-V semiconductors are formed in zinc-blende structure. The feature of zinc-blende structure is the lattice in this form doesn't have inversion

symmetry. So the electrons are exposed to an asymmetric crystal potential during the moving in the lattice. This SO interaction leads to spin-splitting in conduction band and this impact was investigated theoretically by Dresselhaus. So it is known as Dresselhaus SO interaction (Dresselhaus, 1955). The strength of Dresselhaus SO interactions depend only on the atomic elements in the crystal lattice. Another source of SO interaction is confining the motions of electrons in two dimension with an an asymmetric confinement potential. What render important this mechanism is that the asymmetry in the confinement potential can be varied electrostatically, namely the strength of SO interaction can be controlled by gate voltages (Schliemann, Egues, & Loss, 2003). This kind of SO interaction is named Rashba SO interaction (Rashba, 1960; Bychkov & Rashba, 1984).

### 3.3.1 *Rashba Spin-Orbit Interaction*

An asymmetric confining potential consists asymmetry in the band structure and this asymmetry leads to Rashba SO interaction. The structural inversion asymmetry in the confining potential generates electric field which is perpendicular to the two-dimensional electron gas (Wrinkler, 2003). The Hamiltonian which describes Rashba SO interaction is written as (Bychkov et al, 1984).

$$\mathcal{H}_R = \frac{\alpha_R}{\hbar} [\boldsymbol{\sigma} \times (\mathbf{p} + e\mathbf{A})]_z \quad (3.3.1)$$

where  $\boldsymbol{\sigma}$  are the Pauli matrices,  $\mathbf{p}$  is the momentum vector and  $\alpha_R$  is the Rashba parameter and it defines the strength of the interaction and it can be varied by the gate electric field (Zhang et al, 2009).

### 3.3.2 *Dresselhaus Spin-Orbit Interaction*

The source of SO coupling is the bulk inversion asymmetry and it arises from lack of an inversion center in the III-V zinc-blende semiconductors. The inversion symmetry in space and time not only changes wave vector  $\mathbf{k}$  into  $-\mathbf{k}$  but also flips spin. When these two inversion operators are combined two degenerate energy states are

obtained for single particle, namely  $E(\mathbf{k}, \uparrow) = E(-\mathbf{k}, \downarrow)$ . This property is commonly seen in group-IV elements such as diamond, Si, Ge. But the inversion asymmetry does not continue in III-V zinc blende structures and  $E(\mathbf{k}, \uparrow) \neq E(-\mathbf{k}, \downarrow)$ . Bulk inversion asymmetry lifts the spin degeneracy and it firstly was investigated by Dresselhaus (Dresselhaus, 1955). And Dresselhaus SO interaction Hamiltonian is given

$$\begin{aligned} \mathcal{H}_D &= \gamma_D \sum_{c.p.x,y,z} \{ \sigma_x \mathcal{K}_x, \mathcal{K}_y^2 - \mathcal{K}_z^2 \} \\ &= \frac{\beta_D}{\hbar} ((p_x + eA_x) \sigma_x - (p_y + eA_y) \sigma_y) + \gamma_D [ \sigma_x \{ \mathcal{K}_x, \mathcal{K}_y^2 \} - \sigma_y \{ \mathcal{K}_y, \mathcal{K}_x^2 \} ] \end{aligned} \quad (3.3.2)$$

$\gamma_D$  is called Dresselhaus parameter and it depends on the effective width and thickness of the quantum wire and can be varied with a split gate potential that controls the oscillator frequency (Zhang et al, 2009).  $\mathcal{K}$  is the canonical momentum with components  $\mathcal{K} = (\mathcal{K}_x, \mathcal{K}_y, \mathcal{K}_z)$  and it can be written as

$$\begin{aligned} \mathcal{K}_x &= \frac{1}{2} \{ (p_x + eA_x)[(p_y + eA_y)^2 - (p_z + eA_z)^2] + [(p_y + eA_y)^2 - (p_z + eA_z)^2](p_x + eA_x) \} \\ \mathcal{K}_y &= \frac{1}{2} \{ (p_y + eA_y)[(p_z + eA_z)^2 - (p_x + eA_x)^2] + [(p_z + eA_z)^2 - (p_x + eA_x)^2](p_y + eA_y) \} \\ \mathcal{K}_z &= \frac{1}{2} \{ (p_z + eA_z)[(p_x + eA_x)^2 - (p_y + eA_y)^2] + [(p_x + eA_x)^2 - (p_y + eA_y)^2](p_z + eA_z) \} \end{aligned}$$

### 3.4 Zeeman Effect

When an atom placed in a uniform external magnetic field, the energy levels are shifted. This phenomenon is known as the Zeeman effect. The energy splitting occurs because of the interaction of the magnetic moment  $\boldsymbol{\mu}$  of the atom with the magnetic field  $\mathbf{B}$  that slightly shifts the energy of the atomic levels by amount  $\Delta E = -\boldsymbol{\mu} \cdot \mathbf{B}$ . This energy depends on the relative orientation of magnetic moment and the magnetic field (Griffiths, 1994). The Hamiltonian of electron spin in a magnetic field can be written as

$$\mathcal{H}_Z = -\boldsymbol{\mu} \cdot \mathbf{B} = g^* \mu_B \mathbf{S} \cdot \mathbf{B} \quad (3.4.1)$$

where  $\boldsymbol{\mu} = -g^* \mu_B \mathbf{S}$  is magnetic moment and  $\mu_B = e\hbar/2m^*$  is Bohr magneton.

## CHAPTER FOUR

### THEORETICAL BACKGROUND

#### 4.1 Schrödinger Equation

The physical and chemical properties of a matter in any phase and in any form can be exactly determined by solving many-body Schrödinger equation.

$$\mathcal{H}\Psi = E\Psi \quad (4.1.1)$$

It is very excellent that this famous equation includes all the information of any system. When you solve the many-body Schrödinger equation it means that you have everything about the system. But solving the Schrödinger equation for a system of  $N$  interacting particle electrons in an external field is a very difficult problem. Only for a few cases analytical solutions exist and the numerical solutions are limited to very small number of particles. In this case, solving the Schrödinger equation requires some approximation.

#### 4.2 Fundamental Approximations to Schrödinger Equation

##### *4.2.1 Born-Oppenheimer Approximation*

When the motion of electrons is compared with the nuclei, the electrons move faster because of their smaller mass. Electrons follow the motion of drowsy nuclei instantaneously. So assuming the movement of electrons depends on positions of nuclei in a parametric way we can separate the movements of electron and nuclei. This is the foundation of Born-Oppenheimer Approximation. According to the this approximation electron remains in the same stationary state all the time (Born & Oppenheimer, 1927).

This approximation provides freedom for ionic coordinates ( $\mathbf{R}_I$ )s which are taken as the equilibrium position, so the ionic coordinates ( $\mathbf{R}_I$ )s can be taken constant. And

many-body electronic Hamiltonian can be written as

$$\hat{\mathcal{H}} = -\sum_{i=1}^n \frac{\hbar^2}{2m} \nabla_i^2 + e^2 \sum_{i=1}^n \left( \sum_{I=1}^P \frac{-Z_I}{|\mathbf{r}_i - \mathbf{R}_I|} \right) + \frac{e^2}{2} \sum_{i=1}^n \sum_{j \neq i}^n \frac{1}{|\mathbf{r}_i - \mathbf{r}_j|} \quad (4.2.1)$$

where second term yields ionic potential and the third term is the interaction between electrons.

#### 4.2.2 Hartree Approximation

As we see the last term of Equation 4.2.1, the repulsion of electron-electron couples the motion of electrons. This coupling prevents the separation of coordinates. So the solution of many-body Hamiltonian is still difficult problem. To get over this problem in 1928 Hartree proposed that many-electron wave function (electronic wave function) can be written as product one-electron wave functions each of which satisfies one-particle Schrödinger equation in an effective potential (Hartree, 1928).

$$\Phi(\mathbf{R}, \mathbf{r}) = \prod_i \varphi(\mathbf{r}_i) \quad (4.2.2)$$

A single electron feels the effective potential is written

$$V_{eff}^{(i)}(\mathbf{R}, \mathbf{r}) = V(\mathbf{R}, \mathbf{r}) + \int \frac{\sum_{j \neq i}^n \rho_j(\mathbf{r}')}{|\mathbf{r} - \mathbf{r}'|} d\mathbf{r}' \quad (4.2.3)$$

where  $\rho_j(\mathbf{r})$  is the electronic density associated with particle  $j$ .

$$\rho_j(\mathbf{r}) = |\varphi_j(\mathbf{r})|^2 \quad (4.2.4)$$

And Schrödinger equation is

$$\left( -\frac{\hbar^2}{2m} \nabla^2 + V_{eff}^{(i)}(\mathbf{R}, \mathbf{r}) \right) \varphi_i(\mathbf{r}) = \varepsilon_i \varphi_i(\mathbf{r}) \quad (4.2.5)$$

The second term in Equation 4.2.3 yields mean field potential and the third term defines the interactions of one electron with the other electrons in a mean field.  $\varepsilon_i$  is the

energy of  $i$ -th electron. The calculation starts with some approximate orbitals  $\phi_i$  for example obtained from hydrogen atom. All of  $N$  equations are solved and by iterating them new  $N$   $\phi_i$ 's are obtained until the self-consistency is achieved. New orbitals are obtained and according to Hartree's proposal, from these orbitals many-electron wave-function  $\Psi$  is formed and then the total energy  $E$  is calculated. The process is named self-consistent field Hartree approximation. The remarkable point is that the total energy of many-body system is not the sum of  $\epsilon_i$  eigenvalues because the effective potential formalism counts the electron-electron interaction twice (Madelung, 1981). The correct expression of the total energy is

$$E^H = \sum_{i=1}^N \epsilon_i - \frac{1}{2} \int \int \frac{\rho(\mathbf{r})\rho(\mathbf{r}')}{|\mathbf{r}-\mathbf{r}'|} d\mathbf{r}d\mathbf{r}' \quad (4.2.6)$$

where second term is correction due to effective potential.

### 4.2.3 Hartree-Fock Approximation

Hartree approximation, namely single electron wave-function approximation is surely a good idea and many-electron function for all the atom is produced via this approximation. But the function form based on Hartree approximation is essentially wrong and it gives incorrect results because it passes over the fermionic nature of electrons. It can be improved by considering the fermionic features of electrons. In accordance with Pauli exclusion principle if two fermions have all same quantum numbers they cannot occupy the same state. Fock and Slater tried to enhancement Hartree approximation. They exploit the one-electron functions but the total wave function isn't the simple product of the orbitals, it is antisymmetrized sum of all products. It defines a determinant and it is known famous Slater determinant (Slater, 1930).

$$\Psi(\mathbf{R}, \mathbf{r}) = \frac{1}{\sqrt{N!}} \begin{pmatrix} \phi_1(\mathbf{r}_1) & \dots & \phi_1(\mathbf{r}_N) \\ \vdots & \ddots & \vdots \\ \phi_N(\mathbf{r}_1) & \dots & \phi_N(\mathbf{r}_N) \end{pmatrix} \quad (4.2.7)$$

This approximation is called Hartree-Fock approximation and it explains particle exchange (Tongay, 2004). In the absence of many-body correlations, this approximation gives a moderate explanation for inter-atomic bonding. The Hartree-Fock approximation is assumed the starting point of advanced calculations. In general form the Hartree-Fock approximation, which includes an extra term due to the coupling, can be written as

$$\left(-\frac{\hbar^2}{2m}\nabla^2 + V(\mathbf{r})\right)\varphi_j(\mathbf{r}) + e^2 \sum_{k \neq j} \int \frac{|\varphi_k(\mathbf{r}')|^2}{|\mathbf{r} - \mathbf{r}'|} d\mathbf{r}' \varphi_j(\mathbf{r})$$

$$+ e^2 \sum_{k \neq j} \int \frac{\varphi_k^*(\mathbf{r}')\varphi_j(\mathbf{r}')}{|\mathbf{r} - \mathbf{r}'|} d\mathbf{r}' \varphi_k(\mathbf{r}) = E_j \varphi_j(\mathbf{r})$$

This is the Hartree-Fock equation.

### 4.3 Density Functional Theory

Thomas and Fermi suggested that the full electron density was the fundamental variable of the many-body problem and derived a differential equation for density without using the one-electron orbitals. This is known Thomas-Fermi Theory and it precipitated to development of density functional theory (DFT). In density functional theory, the electron density is the quantity of interest.

Calculating the total energy of system composed of N interacting electron in an external field there is a serious problem with taking the correlation effects into account. There exists electron-electron interactions and so the total energy can be written as

$$E = \langle \varphi | \hat{T} + \hat{V} + \hat{V}_{ee} | \varphi \rangle = \langle \varphi | \hat{T} | \varphi \rangle + \langle \varphi | \hat{V} | \varphi \rangle + \langle \varphi | \hat{V}_{ee} | \varphi \rangle \quad (4.3.1)$$

where  $\hat{T}$  is kinetic energy,  $\hat{V}$  the energy arises from external field and  $\hat{V}_{ee}$  is the electron-electron interaction energy.

The kinetic energy term is defined as

$$T = \langle \varphi | -\frac{\hbar^2}{2m} \sum_{i=1}^N \nabla_i^2 | \varphi \rangle = -\frac{\hbar^2}{2m} \int [\nabla_r^2 \rho_1(\mathbf{r}, \mathbf{r}')]_{r=r'} d\mathbf{r} \quad (4.3.2)$$



And the external field energy term can be written as

$$V = \sum_{I=1}^N \langle \varphi | \sum_{i=1}^N v(\mathbf{r}_i - \mathbf{R}_I) | \varphi \rangle = \sum_{i=1}^N \int \rho(\mathbf{r}) v(\mathbf{r} - \mathbf{R}_I) d\mathbf{r} \quad (4.3.3)$$

And lastly the electron-electron interaction term with considering Coulomb interaction is defined

$$V_{ee} = \langle \varphi | \frac{1}{2} \sum_{i=1}^N \sum_{j \neq i}^N \frac{1}{|\mathbf{r}_i - \mathbf{r}_j|} | \varphi \rangle = \int \frac{\rho_2(\mathbf{r}, \mathbf{r}')}{|\mathbf{r} - \mathbf{r}'|} d\mathbf{r} d\mathbf{r}' \quad (4.3.4)$$

where  $\rho_1(\mathbf{r}, \mathbf{r}')$  is one-body density matrix and  $\rho_2(\mathbf{r}, \mathbf{r}')$  is two-body density matrix. In general form p-body density matrix is defined by (Parr & Yang, 1989).

$$\rho_p(x_1, x_2, \dots, x_p, x'_1, x'_2, \dots, x'_p) = \binom{N}{p} \int \varphi_0^*(x_1, x_2, \dots, x_p, \dots, x_N) \varphi_0(x'_1, x'_2, \dots, x'_p, \dots, x_N) dx_{p+1} \dots dx_N \quad (4.3.5)$$

Also two-body density matrix can be defined via two-body correlation function  $g(\mathbf{r}, \mathbf{r}')$

$$\rho_2(\mathbf{r}, \mathbf{r}') = \frac{1}{2} \rho(\mathbf{r}, \mathbf{r}) \rho(\mathbf{r}, \mathbf{r}') g(\mathbf{r}, \mathbf{r}') \quad (4.3.6)$$

In the light of these knowledge electron-electron interaction energy can be redefined

$$V_{ee} = \frac{1}{2} \int \frac{\rho(\mathbf{r}) \rho(\mathbf{r}')}{|\mathbf{r} - \mathbf{r}'|} d\mathbf{r} d\mathbf{r}' + \frac{1}{2} \int \frac{\rho(\mathbf{r}) \rho(\mathbf{r}')}{|\mathbf{r} - \mathbf{r}'|} [g(\mathbf{r}, \mathbf{r}') - 1] d\mathbf{r} d\mathbf{r}' \quad (4.3.7)$$

In the last equation the first term yields to classical electrostatic interaction energy and the second term includes correlation effects. Electrons are fermions so they have antisymmetric wave functions and spatial separation is observed between the electrons with same spin. This separation reduces Coulomb energy and the reduction is called exchange energy. Hartree-Fock approximation allows us calculating the exchange energy. The Coulomb interaction leads to spatial separation between opposite spins. The correlation energy is defined as the difference between the total energy of system and the energy calculated from Hartree-Fock approximation. The total energy of system is

$$E = T + V + J + E_{xc} \quad (4.3.8)$$

where J is internal energy of classic repulsive gas

$$J = \frac{1}{2} \int \frac{\rho(\mathbf{r})\rho(\mathbf{r}')}{|\mathbf{r} - \mathbf{r}'|} d\mathbf{r}d\mathbf{r}' \quad (4.3.9)$$

$E_{xc}$  is the exchange-correlation energy

$$E_{xc} = \frac{1}{2} \int \frac{\rho(\mathbf{r})\rho(\mathbf{r}')}{|\mathbf{r} - \mathbf{r}'|} [g(\mathbf{r}, \mathbf{r}') - 1] d\mathbf{r}d\mathbf{r}' \quad (4.3.10)$$

### 4.3.1 Hohenberg-Kohn Theorems

The idea of electron density is the basic definition which remained unproved for many years. In 1964, Hohenberg-Kohn legitimized the use of electron density as a basic variable. They proved the fact that ground state features are functionals of electron density  $\rho(\mathbf{r})$  and this property constituted the fundamental of modern density functionals methods (Hohenberg & Kohn, 1964). The Hohenberg-Kohn theorem can be explained by two theorems.

**Theorem 1:** The external potential  $V(\mathbf{r})$  is determined, within a trivial additive constant, by the electron density  $\rho(\mathbf{r})$  (Parr et al, 1989).  $\rho$  has the number of electrons knowledge and gives  $V(\mathbf{r})$ , the ground state wave-function  $\Psi$  and all of the electronic properties of the system. It should be note that the external potential  $V(\mathbf{r})$  isn't restricted to Coulomb potentials.

**Theorem 2:** (Variational Principle) The ground state density can be calculated using the variational method involving density instead of wave-functions.

The ground state energy  $E$  can be obtained by solving the Schrödinger equation

$$E = \min \frac{\langle \Psi | H | \Psi \rangle}{\langle \Psi | \Psi \rangle} \quad (4.3.11)$$

The first principle Hohenberg-Kohn theorem is using  $\rho(\mathbf{r})$  instead of  $\Psi(\mathbf{r})$ .  $\rho(\mathbf{r})$  is the ground state density the minimum energy is obtained for a non-degenerate system. And it is written as

$$E_V[\rho] = F[\rho] + \int \rho(\mathbf{r})v(\mathbf{r})d\mathbf{r} \quad (4.3.12)$$

where

$$F[\tilde{\rho}] = \langle \Psi[\rho] | \hat{T} + \hat{U} | \Psi[\rho] \rangle \quad (4.3.13)$$

When you have the  $F[\rho]$  knowledge this means that you have solved many-body Schrödinger equation. There is an important point that  $F[\rho]$  is a universal functional and it depends only on the electron density, not on the external potential so it doesn't require the knowledge of external potential. According to the Hohenberg-Kohn theorem,  $F[\rho]$  is defined as  $F[\rho] = \langle \Psi | \hat{T} + \hat{U} | \Psi \rangle$ ,  $\Psi$  is the ground state wave-function. These two theorems constitute the basis of DFT. When  $F[\rho]$  is known, the electronic ground state density and energy is defined by using DFT. But it shouldn't consider that the DFT is a ground state theory and doesn't include excited states. It is a wrong statement. Because density determines univocally the potential and the many-body wave-functions, which include ground and excited states, and so the many-body Schrödinger equation is solved. Kohn and Sham invented the ground state such a scheme.

### 4.3.2 Kohn-Sham Equations

After Hohenberg-Kohn theorems, Kohn and Sham took to the stage and they proposed their famous theory which computes the main contribution to the kinetic energy functional (Kohn, & Sham, 1965). Their method bases on the non-interacting Kohn-Sham particles which behave as non-interacting electrons. Within Kohn-Sham scheme the system of many interacting electrons can be written as a system of non-interacting Kohn-Sham particles.

The internal electronic energy functional  $F[\rho]$  can be divided into three parts

$$F[\rho] = T[\rho] + J[\rho] + E_{xc}[\rho] \quad (4.3.14)$$

where  $T[\rho]$  is the kinetic energy of non-interacting kinetic energy, namely the kinetic energy of a system consisted of the non-interacting Kohn-Sham particles and  $\rho$  is the particle density of this system,  $J[\rho]$  is the electrostatic energy of a classical repulsive gas and the last term  $E_{xc}[\rho]$  is the exchange-correlation energy. The exchange-

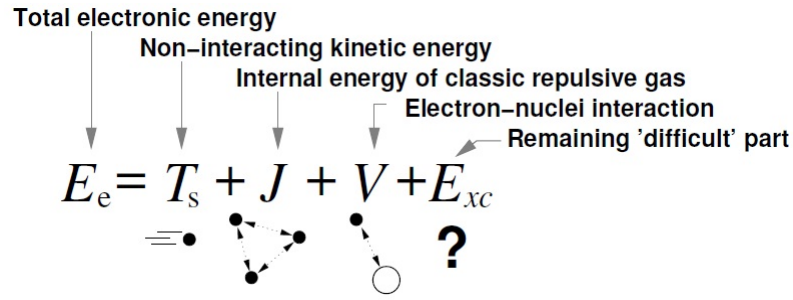


Figure 4.1 The different contributions to the energy in the Kohn-Sham scheme (Armiento, 2005).

correlation energy is defined as

$$E_{xc}[\rho] = F[\rho] - T[\rho] - J[\rho] \quad (4.3.15)$$

Now  $E_{xc}[\rho]$  is the component of  $F[\rho]$  and  $F[\rho]$  includes the non-classical part of potential and kinetic energy related to electron interactions. By this way the total electronic energy is divided into four terms.

$$E = T + J + V + E_{xc} \quad (4.3.16)$$

According to the DFT variational principle the ground state energy is calculated by as

$$E_0 = \min_{\Psi} \langle \Psi | H | \Psi \rangle = \min_{\rho} \min_{\Psi \rightarrow \rho} \langle \Psi | \hat{T} + \hat{U} + \hat{V} | \Psi \rangle = \min_{\rho} (F[\rho] + V[v, \rho]) \quad (4.3.17)$$

where  $v$  is static external potential which originates from the nuclei. The ground state electronic energy can be rewritten with these new quantities

$$E_0 = \min_{\rho} (T[\rho] + J[\rho] + E_{xc}[\rho] + V[v, \rho]) \quad (4.3.18)$$

Energy minimization is written as in the variational calculus

$$\frac{\delta T[\rho]}{\delta \rho} + \frac{\delta E_{xc}[\rho]}{\delta \rho} + \frac{\delta J[\rho]}{\delta \rho} + \frac{\delta V[v, \rho]}{\delta \rho} = 0 \quad (4.3.19)$$

This DFT variational principle can be applied the system which consists of the non-interacting Kohn-Sham particles. The ground state energy  $E_{KS}$  this system is given

as

$$E_{KS} = \min_{\rho} (T[\rho] + V[v_{eff}, \rho]) \quad (4.3.20)$$

$v_{eff}$  is the potential where in the Kohn-Sham particles move. And the minimization of this energy

$$\frac{\delta T[\rho]}{\delta \rho} + \frac{\delta V[v_{eff}, \rho]}{\delta \rho} = 0 \quad (4.3.21)$$

When the interacting and non-interacting systems are compared, Equation 4.3.21 and Equation 4.3.23 shows the same stationary  $\rho$ . By comparing the similarity of the two cases allows us to write

$$\frac{\delta V[v_{eff}, \rho]}{\delta \rho} = \frac{\delta E_{ex}[\rho]}{\delta \rho} + \frac{\delta J[\rho]}{\delta \rho} + \frac{\delta V[\rho]}{\delta \rho} \quad (4.3.22)$$

The functional derivatives of these expressions are

$$v_{eff}(\mathbf{r}) = v_{xc}(\mathbf{r}) + \int \frac{\rho(\mathbf{r}')}{|\mathbf{r} - \mathbf{r}'|} d\mathbf{r}' + v(\mathbf{r}) \quad (4.3.23)$$

$v_{xc}(\mathbf{r})$  yields to exchange-correlation potential and it is defined as

$$v_{xc}(\mathbf{r}) = \frac{\delta E_{ex}[\rho]}{\delta \rho} \quad (4.3.24)$$

If we want to derive a relation between the energies of interacting and non-interacting systems we can write this expression

$$E_0 = E_{KS} - J[\rho] + E_{xc}[\rho] - V[v_{xc}, \rho] \quad (4.3.25)$$

$E_{KS}$  Kohn-Sham functional is the total energy functional

$$E_{KS} = T[\rho] + V[\rho] + J[\rho] + E_{xc}[\rho] \quad (4.3.26)$$

In conclusion, it has been established that the non-interacting Kohn-Sham particle system with  $v_{eff}$  has the same ground state density as the system of fully interacting electrons. As we see the energy of non-interacting particles can be minimized instead of the energy of non-interacting particles. The non-interacting problem can be solved via the solution of separable Schrödinger equation. Kohn-Sham orbital equation is obtained from the separation and this equation determines the one-particle Kohn-Sham

orbitals  $\varphi_i(r)$  and the Kohn-Sham orbital energies  $\varepsilon_i$ ,

$$\left(-\frac{\hbar^2}{2m}\nabla^2 + v_{eff}\right)\varphi_i(\mathbf{r}) = \varepsilon_i\varphi_i(\mathbf{r}) \quad (4.3.27)$$

$\varphi_i(\mathbf{r})$  is the position part of the one-particle wave function which in fact also depends on the spin function. So the one-particle wave function is  $\Psi(\mathbf{r}, \sigma) = \varphi_i(\mathbf{r})\chi_i(\sigma)$  and the ground state wave function of the many independent particle system is given by Slater determinant. The particle of the density is calculated by summing over all occupied spin states.

$$\rho(\mathbf{r}) = \sum_i |\varphi_i(\mathbf{r})|^2 \quad (4.3.28)$$

The total energy of the system is

$$E_{KS} = \sum_i \varepsilon_i \quad (4.3.29)$$

Equation 4.3.29 and Equation 4.3.31 are the famous Kohn-Sham equations and the vital equations of DFT. These equations have difficulty due to the  $v_{eff}$ , it requires unknown density. But we have a chance because the existence of a minimization principle over densities means that the correct electron density  $\rho(\mathbf{r})$  fulfills a stationary condition. The stationary  $\rho(\mathbf{r})$  can be calculated by an iterative scheme. The process starts with a trial density and goes on until self-consistency is achieved.

#### 4.4 Exchange-Correlation Energy

Hohenberg-Kohn and Kohn-Sham theorems reduce many-particle Schrödinger equation into single-particle Schrödinger equation. And these theorems provide that ground state properties are functionals of electron density. But the exchange-correlation part is a problem, it is still unknown.

#### 4.4.1 Local Density Approximation

The local density approximation (LDA) (Jones & Gunnarsan, 1989) is the most commonly used approximation for calculating exchange-correlation energy. It starts from assuming that exchange-correlation energy per particle is a local functional of the electron density. Thus the exchange-correlation energy can be written as the integral of the density and exchange-correlation energy functional.

$$E_{xc}^{LDA}[\rho(\mathbf{r})] = \int \epsilon_{xc}(\rho(\mathbf{r}))\rho(\mathbf{r})d\mathbf{r} \quad (4.4.1)$$

$$\frac{\delta E_{xc}[\rho(\mathbf{r})]}{\delta \rho(\mathbf{r})} = \frac{\partial [\rho(\mathbf{r})\epsilon_{xc}(\rho(\mathbf{r}))]}{\partial \rho(\mathbf{r})} \quad (4.4.2)$$

The exchange-correlation energy per electron at position  $\mathbf{r}$  in inhomogeneous electronic system is equal to the exchange-correlation energy per electron in homogenous electron gas (Payne, Teter, Allan, Arios, & Joannopoulos, 1992).

$$\epsilon_{xc} = \epsilon_{xc}^{hom}[\rho(\mathbf{r})] \quad (4.4.3)$$

Although the exchange-correlation energy per particle is assumed to be local but in fact it is non-local due to inhomogeneities in the electron density. The exchange-correlation energy density depends on the presence of other electrons which encompass the electron at position  $\mathbf{r}$ , through exchange-correlation hole. LDA is a very well approximation because it gives the correct sum rule for the exchange-correlation hole. And it is more useful than other approximations to handle exchange-correlation energy. Although LDA works so well for homogenous system, it tends to fail for systems where large deviations in the electronic density occur.

#### 4.4.2 The Local Spin Density Approximation

Up to now we didn't consider the spin. But the systems which include open electronic shells need better approximations to calculate the exchange-correlation energy. The exchange-correlation functional can be acquired by defining the spin densities  $\rho_{\uparrow}(\mathbf{r})$  the spin-up density and  $\rho_{\downarrow}(\mathbf{r})$  spin-down density. The total density is  $\rho(\mathbf{r}) =$

$\rho_{\uparrow}(\mathbf{r}) + \rho_{\downarrow}(\mathbf{r})$  and the magnetization density is  $\zeta(\mathbf{r}) = (\rho_{\uparrow}(\mathbf{r}) - \rho_{\downarrow}(\mathbf{r}))/\rho(\mathbf{r})$ . The equivalent of the LDA in the spin-polarized systems is the local spin density approximation (LSDA). The exchange-correlation energy with the spin case is (Giuliani & G. Vignale, 2005)

$$E_{xc}^{LSDA}[\rho_{\uparrow}(\mathbf{r}), \rho_{\downarrow}(\mathbf{r})] = \int [\rho_{\uparrow}(\mathbf{r}) + \rho_{\downarrow}(\mathbf{r})] \epsilon_{xc}[\rho_{\uparrow}(\mathbf{r}), \rho_{\downarrow}(\mathbf{r})] \quad (4.4.4)$$

## 4.5 Theoretical Methods

### 4.5.1 Variational Principle

There are some approximations to solve the Schrödinger equation. Variational principle is a well suited approximation to find ground state energy and wave functions. It may be defined that the expectation value of a Hamiltonian  $\mathcal{H}$  is calculated using a trial wave function  $\Psi_T$ , and this value is never lower than the value of the true ground state energy  $E_g$  which is the expectation value of  $\mathcal{H}$  calculated using the true ground state wave function  $\Psi_0$ .

$$E_g \leq \langle \Psi_T | \mathcal{H} | \Psi_T \rangle \equiv \langle \mathcal{H} \rangle \quad (4.5.1)$$

The exact value of ground state energy is calculated by using the exact ground state wave functions.

$$E_g = \frac{\langle \Psi_0 | \mathcal{H} | \Psi_0 \rangle}{\langle \Psi_0 | \Psi_0 \rangle} \quad (4.5.2)$$

The energy associated with the trial wave function is given by,

$$E_T = \frac{\langle \Psi_T | \mathcal{H} | \Psi_T \rangle}{\langle \Psi_T | \Psi_T \rangle} \quad (4.5.3)$$

The variational principle is immensely powerful and easy to use. Even if  $\Psi_T$  is not related to the true wave function, one often gets accurate values for  $E_g$ . The only trouble with this method is that you never know for sure how close you are to the target (Griffiths, 1994).



#### 4.5.2 *Finite Element Method*

Finite Element Method (FEM) is used for numerical calculation of various systems. FEM can be applied to the systems which have the complicate boundary conditions, have not ordered geometry, stationary state, dependence on time and eigenvalue problems. This method is used for the solution of linear and nonlinear problems we face with in liquid mechanics, acoustics, electromagnetism, biomechanics, transfer of heat (Hutton, 2004).

In this method, basis functions are generated by division the domain into a set of simple subdomains. Each subdomain is called finite element or global element. The process of separating the study region to finite number element expresses discontinuity. The point where the elements connect with each other called node. The domain between two nodes is named local element. Gathering of elements, closed to each other, through common boundary provides continuity of the solution.

The approximation of in piece of physical region on the finite elements provides genius, more perfect results than basic approximation functions. The more number of element the more correct and accurate results are obtained. For the generation of algorithm; the domain is discreted, the element interpolation functions are selected, the element equations are determined, the element equations into the system equations are assembled, the boundary conditions are applied to the system equations, the system is solved and any supplemental calculations are performed. In this work, we follow the FEM algorithm which has been developed by Güneş, Urgan and Yeşilgül (Güneş, 2009; Urgan, 2010; Yeşilgül, 2010).

Interpolation is a method of constructing new data points within the range of discrete set of known data points. In the global element, a linear scalar field with d-dimensions can be defined as

$$F(x) = a_0 + a_1x_1 + a_2x_2 + \dots + a_dx_d \quad (4.5.4)$$

at discrete space, where  $i$  is the number of node and  $x(i)$  is the coordinate of node  $F_i = F(x(i))$ .

The notation for a vector or matrix used throughout this work is chosen as follows,

$$\begin{array}{ccc} \text{Matrix} & \text{Column Matrix} & \text{Row Matrix} \\ \{\{A\}\} & \{A\} & \{A\}^T \end{array}$$

$$\{F\}^T = \left( F_1 \ F_2 \ \cdots \ F_{d+1} \right) \quad (4.5.5)$$

$$\{a\}^T = \left( a_0 \ a_1 \ \cdots \ a_d \right) \quad (4.5.6)$$

If we define  $V_d$  as d-dimensional volume element of the global element, scalar field can be written as product of nodes and coefficients

$$\{F\} = \{\{x\}\} \cdot \{a\} \quad (4.5.7)$$

$$\text{Det}(\{\{x\}\}) = d!V_d \quad (4.5.8)$$

The solution of unknown  $a_i$  coefficients in general form is

$$a_i = \frac{1}{d!V_d} (-)^i \begin{vmatrix} F_1 & 1 & x_1(1) & \cdot & x_{i-1}(1) & x_{i+1}(1) & \cdot & x_d(1) \\ F_2 & 1 & x_1(2) & \cdot & x_{i-1}(2) & x_{i+1}(2) & \cdot & x_d(2) \\ F_3 & 1 & x_1(3) & \cdot & x_{i-1}(3) & x_{i+1}(3) & \cdot & x_d(3) \\ \cdot & \cdot & \cdot & \cdot & \cdot & \cdot & \cdot & \cdot \\ \cdot & \cdot & \cdot & \cdot & \cdot & \cdot & \cdot & \cdot \\ F_{d+1} & 1 & x_1(d+1) & \cdot & x_{i-1}(d+1) & x_{i+1}(d+1) & \cdot & x_d(d+1) \end{vmatrix} \quad (4.5.9)$$

From Equation 4.5.4,  $F_i$  can be rewritten in terms of coefficients

$$F(x) = F_1 L_1(x) + F_2 L_2(x) + \cdots + F_{d+1} L_{d+1}(x) \quad (4.5.10)$$

where  $i = 1, 2, \dots, d, d+1$  and  $x = (x_1, x_1, \dots, x_d)$ . There is a new expression area coordinates L. Area coordinates have to satisfy the conditions below.

$$L_i(x(j)) = \delta_{i,j} \quad (4.5.11)$$

$$\sum_{i=1}^{d+1} L_i(x) = 1 \quad (4.5.12)$$

$$\sum_{k=1}^{d+1} L_k(x(i))L_k(x(j)) = \delta_{i,j} \quad (4.5.13)$$

where  $i, j, k = 1, 2, \dots, d, d+1$ ;  $x = (x_1, x_2, \dots, x_d)$ .

And the partial derivative of area coordinates is

$$\frac{\partial L_i(x)}{\partial x(j)} = \frac{1}{d!V_d} (-)^{i-1} (-)^j.$$

$$\begin{vmatrix} 1 & x_1(1) & x_2(1) & \cdot & x_{j-1}(1) & x_{j+1}(1) & \cdot & x_d(1) \\ \cdot & \cdot & \cdot & \cdot & \cdot & \cdot & \cdot & \cdot \\ 1 & x_1(i-1) & x_2(i-1) & \cdot & x_{j-1}(i-1) & x_{j+1}(i-1) & \cdot & x_d(i-1) \\ 1 & x_1(i+1) & x_2(i+1) & \cdot & x_{j-1}(i+1) & x_{j+1}(i+1) & \cdot & x_d(i+1) \\ \cdot & \cdot & \cdot & \cdot & \cdot & \cdot & \cdot & \cdot \\ 1 & x_1(d+1) & x_2(d+1) & \cdot & x_{j-1}(d+1) & x_{j+1}(d+1) & \cdot & x_d(d+1) \end{vmatrix}$$

In one-dimension a global element with 2 nodes

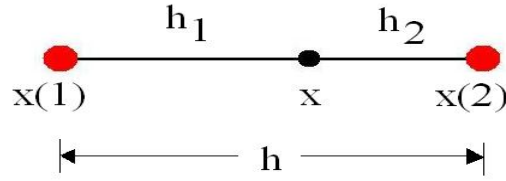


Figure 4.2 A global element with two nodes

$$h_1 = x - x(1), h_2 = x(2) - x, h = x(2) - x(1)$$

$$h = h_1 + h_2$$

$$1 = \frac{h_1}{h} + \frac{h_2}{h}, \quad 1 = L_1 + L_2$$

$$d = 1, V_1 = (x(2) - x(1))$$

$$L_1 = \frac{1}{V_1} \begin{vmatrix} 1 & x \\ 1 & x(2) \end{vmatrix} = \frac{(x(2) - x)}{(x(2) - x(1))} \quad (4.5.14)$$

$$L_2 = \frac{1}{V_1} \begin{vmatrix} 1 & x(1) \\ 1 & x \end{vmatrix} = \frac{(x - x(1))}{(x(2) - x(1))} \quad (4.5.15)$$

Interpolation functions, that span the all space, can be defined in terms of shape functions which span only global elements.

$$N_1(x) = L_1(x), N_2(x) = L_2(x), N_i(x(j)) = \delta_{i,j}, (i, j = 1, 2)$$

Higher order basis in 2-dimension and 3-dimension also can be written but they are not addressed here.

$V_d$  is d-dimensional volume element,

$$\begin{aligned} V_d &= \int dx_1 \int dx_2 \int dx_3 \dots \int dx_d dx_1 dx_2 \dots dx_d \\ &= J \int_0^1 dL_1 \int_0^{1-L_1} dL_2 \int_0^{1-L_1-L_2} dL_3 \dots \int_0^{1-L_1-L_2-\dots-L_{d-1}} dL_d \end{aligned} \quad (4.5.16)$$

constraints on the area coordinates is

$$1 = L_1 + L_2 + \dots + L_d + L_{d+1} \quad (4.5.17)$$

where J is Jacobian

$$V_d = J \frac{1}{d!} \Rightarrow J = d! V_d \quad (4.5.18)$$

In order to apply FEM to the Schrodinger equation, we consider dimensionless one-particle Hamiltonian where  $V(\mathbf{r})$  defines a general potential profile. Solution of  $H\psi = E\psi$  can be achieved by starting a division of the physical region.

If  $N_{tot}$  represents the number of total nodes in meshed domain, and interpolation functions that span the domain are given by set  $\{\phi_n(\mathbf{r})\}$

$$\psi(\mathbf{r}) = \sum_{n=1}^{N_{tot}} \psi_n \phi_n(\mathbf{r}) \quad (4.5.19)$$

$$\phi_i(\mathbf{r}(j)) = \delta_{i,j} \quad (4.5.20)$$

where  $i, j = 1, 2, \dots, N_{tot}$ . Matrix notation of the wave function we search for is

$$\{\phi(\mathbf{r})\}^T = (\phi_1(\mathbf{r}), \phi_2(\mathbf{r}), \phi_3(\mathbf{r}), \dots, \phi_N(\mathbf{r}))$$

$$\{\psi\}^T = (\psi_1, \psi_2, \psi_3, \dots, \psi_N)$$

therefore,

$$\psi(\mathbf{r}) = \{\phi(\mathbf{r})\}^T \cdot \{\psi\}$$

The number of  $N_{tot}$  variation parameter  $\psi_{N_{tot}}$  can be obtained by Galerkin method (Zienkiewicz, Taylor, & Zhu, 2005). The essential principle is to write Schrödinger equation with the wanted wave function  $\psi(\mathbf{r})$ , multiply the equation with its hermitian conjugate from left and integrating the system in related domain to obtain the expression which makes the variation parameters minimum. Using this expression  $\psi(\mathbf{r})^\dagger = \{\psi\}^\dagger \cdot \{\phi(\mathbf{r})\}$  Galerkin is

$$G = \int_{\Omega} \psi(\mathbf{r})^\dagger (H - \epsilon) \psi(\mathbf{r}) d\Omega \quad (4.5.21)$$

By the wave function to find and it's hermitian conjugate, Galerkin becomes

$$G = \{\psi\}^\dagger \cdot \left[ \int_{\Omega} \{\phi(\mathbf{r})\} (H - \epsilon) \{\phi(\mathbf{r})\}^T d\Omega \right] \cdot \{\psi\} \quad (4.5.22)$$

The wave function family  $(\psi, \psi^\dagger)$  for a minimum G gives the energy eigenvalues  $\partial G / \partial \{\psi\}^\dagger = 0$  therefore,

$$\left[ \int_{\Omega} \{\phi\} (H - \epsilon) \{\phi\}^T d\Omega \right] \cdot \{\psi\} = 0 \quad (4.5.23)$$

Before the writing down Hamiltonian explicitly, the contribution of kinetic term can be investigated. After the first integration on the kinetic part of Hamiltonian becomes

$$- \int_{\Omega} \{\phi\} \cdot \nabla_d^2 \{\phi\}^T \cdot d\Omega = \int_{\Omega} \nabla_d \{\phi\} \cdot \nabla_d \{\phi\}^T \cdot d\Omega - \int_{\Gamma} \{\phi\} (\nabla_d \{\phi\}^T) \cdot d\Gamma \quad (4.5.24)$$

The wanted wave function and its conjugate must be zero at the boundary of the system so the second terms doesn't give any contribution. The explicit expression of the Hamiltonian is written in the definition of the variation of the G

$$\left[ \int_{\Omega} d\Omega \left[ \frac{1}{2} \nabla_d \{\phi\} \cdot \nabla_d \{\phi\}^T + \{\phi\} V(\mathbf{r}) \{\phi\}^T \right] \right] \cdot \{\psi\} = \epsilon \left[ \int_{\Omega} d\Omega \{\phi\} \{\phi\}^T \right] \quad (4.5.25)$$

Equation 4.5.33 can be rewritten in a matrix form

$$\{\{K\}\} \cdot \{\psi\} = \varepsilon \{\{M\}\} \cdot \{\psi\} \quad (4.5.26)$$

where  $\{\{K\}\}$  is stiffness matrix and  $\{\{M\}\}$  is mass matrix. The explicit expressions are

$$\{\{K\}\} = \int_{\Omega} d\Omega \left[ \frac{1}{2} \nabla_d \{\phi\} \cdot \nabla_d \{\phi\}^T + \{\phi\} V(\mathbf{r}) \{\phi\}^T \right] \quad (4.5.27)$$

$$\{\{M\}\} = \int_{\Omega} d\Omega \{\phi\} \{\phi\}^T \quad (4.5.28)$$

The integrals over the whole work space can be re-described as the summation of the integrals over the divided work space elements.

$$\int_{\Omega} d\Omega = \sum_{e=1}^{N_e} \int_{\Omega_e} d\Omega_e \quad (4.5.29)$$

and than global element stiffness matrix  $\{\{k_e\}\}$  and global element mass matrix  $\{\{m_e\}\}$  are

$$\begin{aligned} \{\{k_e\}\} &= \int_{\Omega_e} d\Omega_e \left[ \frac{1}{2} \nabla_d \{N\} \cdot \nabla_d \{N\}^T + \{N\} V \{N\}^T \right] \\ \{\{K_e\}\} &= \sum_{e=1}^{N_e} \{\{k_e\}\} \end{aligned} \quad (4.5.30)$$

$$\{\{m_e\}\} = \int_{\Omega_e} d\Omega_e \{N\} \{N\}^T \quad (4.5.31)$$

$$\{\{M_e\}\} = \sum_{e=1}^{N_e} \{\{m_e\}\} \quad (4.5.32)$$

where  $\{\phi\}$  is all space interpolation functions and  $\{N\}$  is global element interpolation functions or Shape functions.

### *Finite Element Analysis for Coupled Systems*

We used the notation for the coupled systems that given Table 4.1 and we exploits the Sarikurt's notes (personal communication, 2011).

Table 4.1 The notation for the coupled systems

	FEM	Coupled System
Matrix	$\{\{X\}\}$	$\overline{\overline{X}}$
Column Matrix	$\{X\}$	$\overline{X}$
Row Matrix	$\{X\}^T$	$\overline{X}^T$

Now, we focus on the solution of a classical Hamiltonian for coupled systems is given as

$$\overline{\overline{\mathcal{H}}} = \overline{\overline{\mathcal{H}}}_A + \overline{\overline{\mathcal{H}}}_{BP\xi} + \overline{\overline{\mathcal{H}}}_{CP\xi}^2 \quad (4.5.33)$$

where  $p_\xi = \frac{1}{i} \frac{\partial}{\partial \xi}$  is the dimensionless canonical momentum. The Hamiltonian in quantum mechanical formulation is

$$\overline{\overline{\mathcal{H}}} = \sum_{n=0}^{\infty} \left\{ \frac{1}{n!} \frac{\partial^n \overline{\overline{\mathcal{H}}}}{\partial p_\xi^n} \Big|_{p_\xi=0}, p_\xi^n \right\} = \{\overline{\overline{\mathcal{H}}}_A, 1\} + \{\overline{\overline{\mathcal{H}}}_B, p_\xi\} + \{\overline{\overline{\mathcal{H}}}_C, p_\xi^2\} \quad (4.5.34)$$

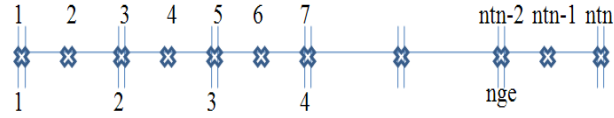
Specify to define

$$\begin{aligned} \{A, B\} &= \frac{1}{2}(AB + BA) \\ \{\overline{\overline{\mathcal{H}}}_A, 1\} &= \frac{1}{2}(\overline{\overline{\mathcal{H}}}_A \cdot 1 + 1 \cdot \overline{\overline{\mathcal{H}}}_A) = \overline{\overline{\mathcal{H}}}_A \\ \{\overline{\overline{\mathcal{H}}}_B, p_\xi\} &= \frac{1}{2}(\overline{\overline{\mathcal{H}}}_{BP\xi} + p_\xi \overline{\overline{\mathcal{H}}}_B) \\ \{\overline{\overline{\mathcal{H}}}_C, p_\xi^2\} &= \frac{1}{2}(\overline{\overline{\mathcal{H}}}_{CP\xi}^2 + p_\xi^2 \overline{\overline{\mathcal{H}}}_C) = p_\xi \overline{\overline{\mathcal{H}}}_{CP\xi} + \frac{1}{2}[\overline{\overline{\mathcal{H}}}_C, p_\xi], p_\xi \end{aligned}$$

Finally the Hamiltonian is obtained

$$\overline{\overline{\mathcal{H}}} = \overline{\overline{\mathcal{H}}}_A + \frac{1}{2}(\overline{\overline{\mathcal{H}}}_{BP\xi} + p_\xi \overline{\overline{\mathcal{H}}}_B) + p_\xi \overline{\overline{\mathcal{H}}}_{CP\xi} + \frac{1}{2}[\overline{\overline{\mathcal{H}}}_C, p_\xi], p_\xi \quad (4.5.35)$$

Within the FEM scheme, the approximate solution is found in the finite dimension function space where the domain is divided into meshes.



$ngen$  : Number of nodes in global element

$nge$  : Number of global element

$ntn$  : Number of total nodes ( $ntn = nge \cdot (ngen - 1) + 1$ )

$nc$  : Number of coupling

$N(\xi)$  : Basis functions in global element

$\mathbb{N}(\xi)$  : Basis functions in whole space

The wave function for  $nc$  coupled band system and the wave function of set of basis functions are given as

$$\chi_1(\xi) = \sum_{i=1}^{ntn} \chi_{i1}(\xi) \mathbb{N}_i(\xi)$$

$$\chi_2(\xi) = \sum_{i=1}^{ntn} \chi_{i2}(\xi) \mathbb{N}_i(\xi)$$

⋮

⋮

⋮

$$\chi_{nc}(\xi) = \sum_{i=1}^{ntn} \chi_{i(nc)}(\xi) \mathbb{N}_i(\xi)$$

The wave function can be shown in matrix notation

$$\bar{\chi}(\xi) = \left\{ \mathbb{N}(\xi) \bar{I} \right\}^\dagger \{ \bar{\chi} \} \quad (4.5.36)$$

$$\bar{\chi}^\dagger(\xi) = \left( \chi_1^\dagger(\xi), \chi_2^\dagger(\xi), \dots, \chi_{nc}^\dagger(\xi) \right) = \{ \bar{\chi} \}^\dagger \left\{ \mathbb{N}(\xi) \bar{I} \right\} \quad (4.5.37)$$

Therefore,  $ntn$  variational parameters ( $\chi_{nc}$ ) which are desired to get can obtain with "Galerkin's Method".

$$G = \{ \bar{\chi} \}^\dagger \left[ \int_{\xi_i}^{\xi_f} d\xi \{ \bar{\mathbb{N}}(\xi) \} \left( \bar{\mathcal{H}} - \epsilon \bar{I} \right) \{ \mathbb{N}(\xi) \}^\dagger \right] \{ \bar{\chi} \} \quad (4.5.38)$$



The functions  $\{\overline{\mathcal{X}}(\xi), \overline{\mathcal{X}}^\dagger(\xi)\}$  which minimalizes the G integration minimalizes the energy.

$$\frac{\partial G}{\partial \{\overline{\mathcal{X}}\}^\dagger} = 0 \quad \Rightarrow \quad \left[ \int_{\xi_i}^{\xi_f} d\xi \{\overline{\mathbb{N}}(\xi)\} (\overline{\mathcal{H}} - \varepsilon \overline{\mathbb{I}}) \{\mathbb{N}(\xi)\}^\dagger \right] \{\overline{\mathcal{X}}\} = 0 \quad (4.5.39)$$

$$\left[ \int_{\xi_i}^{\xi_f} d\xi \{\overline{\mathbb{N}}(\xi)\} \overline{\mathcal{H}} \{\mathbb{N}(\xi)\}^\dagger \right] \{\overline{\mathcal{X}}\} = \varepsilon \left[ \int_{\xi_i}^{\xi_f} d\xi \{\overline{\mathbb{N}}(\xi)\} \{\mathbb{N}(\xi)\}^\dagger \right] \{\overline{\mathcal{X}}\} \quad (4.5.40)$$

With the new presentation the generalized eigenvalue equation is obtained.

$$\{\{\overline{\mathbb{K}}\}\} \{\overline{\mathcal{X}}\} = \varepsilon \{\{\overline{\mathbb{M}}\}\} \{\overline{\mathcal{X}}\} \quad (4.5.41)$$

Stiffness and mass matrices under this new notation are

$$\{\{\overline{\mathbb{K}}\}\} = \int_{\xi_i}^{\xi_f} d\xi \{\overline{\mathbb{N}}(\xi)\} \overline{\mathcal{H}} \{\overline{\mathbb{N}}(\xi)\}^\dagger \quad (4.5.42)$$

$$\{\{\overline{\mathbb{M}}\}\} = \int_{\xi_i}^{\xi_f} d\xi \{\overline{\mathbb{N}}(\xi)\} \{\overline{\mathbb{N}}(\xi)\}^\dagger \quad (4.5.43)$$

The Hamiltonian is

$$\overline{\mathcal{H}} = \overline{\mathcal{H}}_A + \frac{1}{2} \left( \overline{\mathcal{H}}_{BP\xi} + p_\xi \overline{\mathcal{H}}_B \right) + p_\xi \overline{\mathcal{H}}_{CP\xi} \quad (4.5.44)$$

## CHAPTER FIVE FORMALISM

### 5.1 System and Its Variables

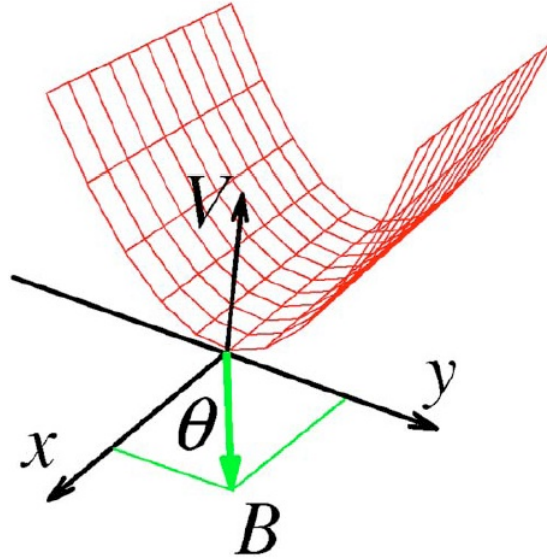


Figure 5.1 Schematic representation of quantum wire (Serra, Sanchez, & Lopez, 2005).

The aim of this thesis is to investigate theoretically the ground state electronic structure of a parabolically confined quantum wire subjected to an in-plane magnetic field, including both Rashba and Dresselhaus spin-orbit interactions and exchange-correlation effects. We consider a parabolic confinement in the  $y$ -direction and free motion along the  $x$ -direction. The electrons are treated within the effective mass approximation, dielectric constant model in two-dimensions where the motion is restricted to the  $xy$  plane as seen in Figure 5.1. In fact the structure is not two-dimensional, but general acceptance is that if the confinement in the perpendicular direction is very strong, the system catches the fundamental physics features of two-dimensional models. In this study, the confinement is strong enough to accept the system in two-dimensions. We use a finite-temperature formalism as a numerical trick in order to avoid the troublesome evaluation of the band occupations at zero temperature.  $T$  has been chosen small enough so the results are the  $T = 0$  results.

The wave function  $\psi_\alpha$  includes both spatial and spinor wave functions.

$$\begin{aligned} \psi_\alpha &\rightarrow \psi_{\sigma,n,\mathbf{k}}(\mathbf{r}) \\ \psi_{\sigma,n,\mathbf{k}}(\mathbf{r}) &= \frac{e^{ikx}}{\sqrt{L}} \begin{pmatrix} \varphi_{n,k}(y,\uparrow) \\ \varphi_{n,k}(y,\downarrow) \end{pmatrix} \end{aligned} \quad (5.1.1)$$

where  $\varphi_{n,k}$  defines the spinor function. The system has translational invariance along the x axis so we can introduce a continuous wave number k which is a good quantum number. The index  $n = 1, 2, 3, \dots$  takes integer numbers and labels different energy subbands. Through this study  $(n, k)$  is used as quantum labels. The advantage of this labeling there is no spin label for the subbands and it satisfies Kohn-Sham spinorial equation.

The Kohn-Sham Hamiltonian of the system is

$$\mathcal{H}_{KS}\psi = \varepsilon\psi \quad (5.1.2)$$

To solve the Kohn-Sham Hamiltonian electron density and spin magnetization must be determined therefore the thermal occupation of each single electron Kohn-Sham orbital must be defined at a given temperature T and chemical potential  $\mu$ . To define the occupation of each  $(n, k)$  state Fermi function is defined.

$$f_\beta(\varepsilon, \mu) = \frac{1}{(1 + e^{\beta(\varepsilon - \mu)})} \quad (5.1.3)$$

where  $\beta = k_B T$  and  $\mu$  is chemical potential. In general form the particle density can be written as the function of chemical potential, temperature and position.

$$\rho(\mu, \beta; \mathbf{r}) = \sum_{\alpha} f_\beta(E_\alpha, \mu) |\psi_\alpha(\mathbf{r})|^2 \quad (5.1.4)$$

At zero temperature  $T = 0$ , the chemical potential is equal to the Fermi energy  $\mu(T = 0) = E_F$ .

$$\rho(\mu, \beta; \mathbf{r}) = \int^{E_F} dE f_\beta(E_\alpha, \mu) D(E; \mathbf{r}) \quad (5.1.5)$$

The equivalence of these two equations we can write local density of states  $D(E; \mathbf{r})$ .

$$D(E; \mathbf{r}) = \sum_{\alpha} \delta(E - E_{\alpha}) |\psi_{\alpha}(\mathbf{r})|^2 \quad (5.1.6)$$

The electron density is written as

$$\rho(\mu, \beta; \mathbf{r}) = \sum_n \frac{L}{2\pi} \int dk \langle \psi_{\sigma, n, k} | \delta(r_i - r) | \psi_{\sigma, n, k} \rangle_{r_i} f_{\mu}(\epsilon_{nk}) \quad (5.1.7)$$

where  $L/2\pi$  arises from box quantization. In this system the electron density depends on  $y$  and it can be written as

$$\rho(y) = \sum_n \sum_k f_{\beta}(\epsilon_{nk}, \mu) \frac{1}{L} (|\varphi_{nk}(y, \uparrow)|^2 + |\varphi_{nk}(y, \downarrow)|^2) \quad (5.1.8)$$

Summation over  $k$  can be transformed to an integration by using the fact  $k.L = 2\pi n$  that leads to

$$\rho(y) = \sum_n \frac{1}{2\pi} \int dk (|\varphi_{nk}(y, \uparrow)|^2 + |\varphi_{nk}(y, \downarrow)|^2) f_{\beta}(\epsilon_{nk}) \quad (5.1.9)$$

The one-dimensional electron density along the quantum wire is the integral of  $\rho(y)$  over  $y$ .

$$\rho_{1D} = \int dy \rho(y) \quad (5.1.10)$$

We can define spin magnetization

$$m_a(\mu, r) = \sum_n \frac{L}{2\pi} \int dk \langle \psi_{nk} | \delta(r_i - r) \sigma_a | \psi_{nk} \rangle_{r_i} f_{\beta}(\epsilon_{nk}, \mu) \quad (5.1.11)$$

By using Pauli spin matrices, magnetization along each direction can be calculated as follows

$$\begin{aligned} m_x(\mu, r) &= \sum_n \frac{L}{2\pi} \int dk \langle \psi_{nk} | \delta(r_i - r) \sigma_x | \psi_{nk} \rangle_{r_i} f_{\beta}(\epsilon_{nk}, \mu) \\ m_x(y) &= \sum_n \frac{1}{2\pi} \int dk 2 \operatorname{Re}[\varphi_{nk}^*(y, \uparrow) \varphi_{nk}(y, \downarrow)] f_{\beta}(\epsilon_{nk}) \\ m_y(\mu, r) &= \sum_n \frac{L}{2\pi} \int dk \langle \psi_{nk} | \delta(r_i - r) \sigma_y | \psi_{nk} \rangle_{r_i} f_{\beta}(E(n, k)) \end{aligned} \quad (5.1.12)$$

$$m_y(y) = \sum_n \frac{1}{2\pi} \int dk 2\text{Im}[\varphi_{nk}^*(y, \uparrow) \varphi_{nk}(y, \downarrow)] f_\beta(\epsilon_{nk}) \quad (5.1.13)$$

$$m_z(\mu, r) = \sum_n \frac{L}{2\pi} \int dk \langle \psi_{nk} | \delta(r_i - r) \sigma_z | \psi_{nk} \rangle_{r_i} f_\beta(E(n, k))$$

$$m_z(y) = \sum_n \frac{1}{2\pi} \int dk (|\varphi_{nk}(y, \uparrow)|^2 - |\varphi_{nk}(y, \downarrow)|^2) f_\beta(\epsilon_{nk}) \quad (5.1.14)$$

## 5.2 Kohn-Sham Hamiltonian

So as to identify the effects of SO interactions and exchange-correlation, we split the Kohn-Sham Hamiltonian into pieces. First of them  $\mathcal{H}_0$  consists of the kinetic and confinement terms, SO Hamiltonian  $\mathcal{H}_R + \mathcal{H}_D$  defines Rashba and Dresselhaus SO interactions, respectively, and the third one  $\mathcal{H}_Z$  the Zeeman effect contribution arising from an in-plane magnetic field applied with an arbitrary orientation. The last term in the Hamiltonian is devoted to the exchange-correlation energy.

The applied in-plane magnetic field is

$$\mathbf{B} = B(\cos \phi_B \mathbf{u}_x + \sin \phi_B \mathbf{u}_y) \quad (5.2.1)$$

where  $\phi_B$  denotes the azimuthal angle.

We can write explicitly

$$\mathcal{H} = \mathcal{H}_0 + \mathcal{H}_Z + \mathcal{H}_R + \mathcal{H}_D + V^{xc} \quad (5.2.2)$$

$$\mathcal{H}_0 = \frac{p_x^2 + p_y^2}{2m^*} + \frac{1}{2} m^* \omega_0^2 y^2 \quad (5.2.3)$$

$$\mathcal{H}_Z = g^* \mu_s \mathbf{B} \cdot \mathbf{S} \quad (5.2.4)$$

$$\mathcal{H}_R = \frac{\alpha_R}{\hbar} (\boldsymbol{\sigma} \times \mathbf{p})_z \quad (5.2.5)$$

$$\mathcal{H}_D = \gamma_D \sum_{x,y,z} \{ \sigma_x \kappa_x, \kappa_y^2 - \kappa_z^2 \} \quad (5.2.6)$$

We solve the Kohn-Sham Hamiltonian with FEM and to do this we scaled the Hamiltonian. We used the harmonic oscillator length  $b_0 = \sqrt{\frac{\hbar}{m^* \omega_0}}$  and the energies are in  $\hbar \omega_0$  units. We also defined some terms to make the hamiltonian dimensionless.  $\mathcal{K}_0 = k_x b_0$ ,

$y = \xi b_0$ ,  $\frac{d}{dy} = \frac{1}{b_0} \frac{d}{d\xi} = \frac{1}{b_0} D_\xi$ ,  $\frac{d^2}{dy^2} = \frac{1}{b_0^2} \frac{d^2}{d\xi^2} = \frac{1}{b_0^2} D_\xi^2$ ,  $p_\xi = \frac{1}{i} \frac{d}{d\xi} = \frac{1}{i} D_\xi$ ;  $D_\xi = ip_\xi$ ;  $D_\xi^2 = -p_\xi^2$  where  $p_\xi$  is dimensionless momentum.

*Kinetic energy and confinement term*

$$\begin{aligned} \mathcal{H}_0 &= \frac{p_x^2 + p_y^2}{2m^*} + \frac{1}{2} m^* \omega_0^2 y^2 \\ &= \frac{\hbar^2 k_x^2}{2m^*} - \frac{\hbar^2}{2m^*} \frac{d^2}{dy^2} + \frac{1}{2} m^* \omega_0^2 y^2 \\ \frac{\mathcal{H}_0}{\hbar\omega_0} &= \left[ \frac{1}{2} p_\xi^2 + \frac{1}{2} \mathcal{H}_0^2 + \frac{1}{2} \xi^2 \right] \sigma_0 \end{aligned} \quad (5.2.7)$$

*Zeeman term*

$$\mathcal{H}_Z = g^* \mu_s \mathbf{B} \cdot \mathbf{S} = \frac{1}{2} g^* \mu_B B (\cos \phi_B \sigma_x + \sin \phi_B \sigma_y)$$

$$\mathcal{H}_Z = \frac{1}{2} g^* \mu_B B (\cos \phi_B \sigma_x + \sin \phi_B \sigma_y) = \hbar\omega_0 \frac{1}{2} \left( \underbrace{\frac{1}{\hbar\omega_0} g^* \mu_B B}_{\mathcal{B}} \right) (\cos \phi_B \sigma_x + \sin \phi_B \sigma_y)$$

where  $\omega_c = eB/m^*$

$$\frac{1}{\hbar\omega_0} g^* \mu_B B = \mathcal{B} = \frac{1}{\hbar\omega_0} g^* \left( \frac{e\hbar}{2m_e} \right) \left( \frac{m^* \omega_c}{e} \right) = g^* \frac{1}{2} \frac{m^*}{m_e} \frac{\omega_c}{\omega_0}$$

$m^*/m_e = m_0$

$$\mathcal{B} = g^* \frac{1}{2} m_0 \frac{\omega_c}{\omega_0}$$

$$\frac{\mathcal{H}_Z}{\hbar\omega_0} = \frac{1}{2} \mathcal{B} (\cos \phi_B \sigma_x + \sin \phi_B \sigma_y) \quad (5.2.8)$$

*Rashba SO term*

$$\begin{aligned} \mathcal{H}_R &= \frac{\alpha_R}{\hbar} (\boldsymbol{\sigma} \times \mathbf{p})_z \\ &= \frac{\alpha_R}{\hbar} (p_y \sigma_x - p_x \sigma_y) = \frac{\alpha_R}{\hbar} \left( -i\hbar \frac{d}{dy} \sigma_x - \hbar k_x \sigma_y \right) \\ \frac{\mathcal{H}_R}{\hbar\omega_0} &= \frac{\alpha_R}{\underbrace{b_0 \hbar \omega_0}} (\sigma_x p_\xi - \sigma_y \mathcal{H}_0) \end{aligned}$$

$$\eta_R = \frac{\alpha_R}{b_0 \hbar \omega_0}$$

$$\frac{\mathcal{H}_R}{\hbar \omega_0} = \eta_R (\sigma_x p_\xi - \sigma_y \mathcal{K}_0)$$

$\Delta_{SO}^R$  is the characteristic Rashba SO energy

$$\Delta_{SO}^R = \frac{m^* \alpha_R^2}{2 \hbar^2} = \frac{m^*}{2 \hbar^2} \eta_R^2 \hbar^2 \omega_0^2 b_0^2 = \frac{m^*}{2} \eta_R^2 \omega_0^2 \frac{\hbar}{m^* \omega_0} = \frac{1}{2} \eta_R^2 \hbar \omega_0$$

$$\frac{\Delta_{SO}^R}{\hbar \omega_0} = \frac{1}{2} \eta_R^2$$

### *Dresselhaus SO term*

$$\mathcal{H}_D = \gamma_D \sum_{x,y,z} \{ \sigma_x \kappa_x, \kappa_y^2 - \kappa_z^2 \}$$

$$\mathcal{H}_D = \frac{\beta_D}{\hbar} (p_x \sigma_x - p_y \sigma_y) + \gamma_D [ \sigma_x \{ \kappa_x, \kappa_y^2 \} - \sigma_y \{ \kappa_y, \kappa_x^2 \} ]$$

Dresselhaus SO interaction term consists of two parts, linear and cubic Dresselhaus SO interactions.

### *Linear Dresselhaus SO term*

$$\mathcal{H}_{D1} = \frac{\beta_D}{\hbar} (p_x \sigma_x - p_y \sigma_y) = \frac{\beta_D}{\hbar} \left( \hbar k_x \sigma_x - \frac{\hbar}{i} \frac{d}{dy} \sigma_y \right)$$

$$\frac{\mathcal{H}_{D1}}{\hbar \omega_0} = \frac{\beta_D}{\hbar \omega_0 b_0} (\mathcal{K}_0 \sigma_x - p_\xi \sigma_y)$$

$$\eta_{D1} = \frac{\beta_D}{\hbar \omega_0 b_0}$$

$$\frac{\mathcal{H}_{D1}}{\hbar \omega_0} = \eta_{D1} (\mathcal{K}_0 \sigma_x - p_\xi \sigma_y)$$

$$\beta_D = \hbar \gamma_D \langle \zeta | \kappa_z^2 | \zeta \rangle$$

$$\eta_{D1} = \frac{1}{\hbar \omega_0 b_0} \hbar \gamma_D \langle \zeta | \kappa_z^2 | \zeta \rangle = \frac{\gamma_D}{\omega_0 b_0} (\overline{\kappa_z^2})$$

$$\kappa_z = \frac{\hbar}{i} \frac{d}{dz}, \quad z = b_0 \tilde{z}$$

$$\kappa_z = \frac{\hbar}{i} \frac{d}{dz} = \frac{\hbar}{i} \frac{1}{b_0} \frac{d}{d\tilde{z}} = \frac{\hbar}{b_0} \mathbf{K}_z$$

$$\eta_{D1} = \frac{1}{\omega_0 b_0} \gamma_D \left( \frac{\hbar^2}{b_0^2} \mathbf{K}_z^2 \right)$$

$$\eta_{D1} = \left( \frac{m^* \hbar}{b_0} \right) \gamma_D \overline{\mathbf{K}_z^2}$$

$\Delta_{SO}^{D1}$  is the Dresselhaus SO interaction energy

$$\Delta_{SO}^{D1} = \frac{m^*}{2\hbar^2} \eta_{D1}^2 \hbar^2 \omega_0^2 b_0^2 = \frac{m^*}{2} \eta_{D1}^2 \omega_0^2 \frac{\hbar}{m^* \omega_0} = \frac{1}{2} \eta_{D1}^2 \hbar \omega_0$$

$$\frac{\Delta_{SO}^{D1}}{\hbar \omega_0} = \frac{1}{2} \eta_{D1}^2$$

*Cubic Dresselhaus SO term*

$$\mathcal{H}_{D2} = \gamma_D [\sigma_x \{ \kappa_x, \kappa_y^2 \} - \sigma_y \{ \kappa_y, \kappa_x^2 \}] = \gamma_D [\sigma_x \{ p_x, p_y^2 \} - \sigma_y \{ p_y, p_x^2 \}]$$

$$= \gamma_D \left[ \sigma_x \left\{ \hbar k_x, \left( \frac{\hbar}{i} \frac{d}{dy} \right)^2 \right\} - \sigma_y \left\{ \left( \frac{\hbar}{i} \frac{d}{dy} \right), (\hbar k_x)^2 \right\} \right]$$

$$= \gamma_D \left( \frac{\hbar}{\omega_0} \right)^3 \left[ -\sigma_x \{ \mathcal{K}_0, D_\xi^2 \} + i \sigma_y \{ D_\xi, \mathcal{K}_0^2 \} \right]$$

$$\frac{\hbar^3}{b_0^3} = \frac{\hbar^3}{\frac{\hbar}{m^* \omega_0} b_0} = \frac{\hbar^2 m^* \omega_0}{b_0}$$

$$\mathcal{H}_{D2} = \gamma_D \frac{\hbar^2 m^* \omega_0}{b_0} \left[ \sigma_x \{ \mathcal{K}_0, -p_\xi^2 \} + i \sigma_y \{ ip_\xi, \mathcal{K}_0^2 \} \right]$$

$$\frac{\mathcal{H}_{D2}}{\hbar \omega_0} = \underbrace{\gamma_D \frac{\hbar m^*}{b_0}} \left[ \sigma_x \{ \mathcal{K}_0, p_\xi^2 \} - \sigma_y \{ p_\xi, \mathcal{K}_0^2 \} \right]$$

$$\eta_{D2} = \gamma_D \frac{\hbar m^*}{b_0}$$

$$\frac{\mathcal{H}_{D2}}{\hbar \omega_0} = \eta_{D2} \left[ \sigma_x \{ \mathcal{K}_0, p_\xi^2 \} - \sigma_y \{ p_\xi, \mathcal{K}_0^2 \} \right]$$

$$\eta_{D1} = \eta_{D2} \overline{\mathbf{K}_z^2}$$



Total Dresselhaus SO term

$$\frac{\mathcal{H}_D}{\hbar\omega_0} = \sigma_x \left[ \eta_{D1} + \eta_{D2} \{ \mathcal{K}_0, p_\xi^2 \} \right] - \sigma_y \left[ \eta_{D1} + \eta_{D2} \{ p_\xi, \mathcal{K}_0^2 \} \right] \quad (5.2.9)$$

Finally we get the scaled Hamiltonian

$$\begin{aligned} \frac{\mathcal{H}_0}{\hbar\omega_0} &= \left[ \frac{1}{2} p_\xi^2 + \frac{1}{2} \mathcal{K}_0^2 + \frac{1}{2} \xi^2 \right] \sigma_0 \\ \frac{\mathcal{H}_Z}{\hbar\omega_0} &= \frac{1}{2} \mathcal{B} (\cos \phi_B \sigma_x + \sin \phi_B \sigma_y) \\ \frac{\mathcal{H}_R}{\hbar\omega_0} &= \eta_R (\sigma_x p_\xi - \sigma_y \mathcal{K}_0) \\ \frac{\mathcal{H}_D}{\hbar\omega_0} &= \sigma_x \left[ \eta_{D1} + \eta_{D2} \{ \mathcal{K}_0, p_\xi^2 \} \right] - \sigma_y \left[ \eta_{D1} + \eta_{D2} \{ p_\xi, \mathcal{K}_0^2 \} \right] \end{aligned}$$

We need to Hamiltonian in quantum mechanical form because the solution in FEM requires it.

$$\mathcal{H} = \mathcal{H}_A + \mathcal{H}_B p_\xi + \mathcal{H}_C p_\xi^2$$

$$\mathcal{H} = \sum_0^\infty \left\{ \frac{1}{n!} \frac{\partial^n \mathcal{H}}{\partial p_\xi^n} \Big|_{p_\xi=0}, p_\xi^n \right\} = \{ \mathcal{H}_A, 1 \} + \{ \mathcal{H}_B, p_\xi \} + \{ \mathcal{H}_C, p_\xi^2 \}$$

$$\mathcal{H}_A = \mathcal{H} \Big|_{p_\xi=0} = \left[ \frac{1}{2} \mathcal{K}_0^2 + \frac{1}{2} \xi^2 \right] \sigma_0 + \frac{1}{2} \mathcal{B} (\cos \phi_B \sigma_x + \sin \phi_B \sigma_y) - \eta_R \sigma_y \mathcal{K}_0 + \eta_{D1} \sigma_x \mathcal{K}_0$$

$$\mathcal{H}_B = \frac{1}{1!} \frac{\partial \mathcal{H}}{\partial p_\xi} \Big|_{p_\xi=0} = \left[ p_\xi \sigma_0 + \eta_R \sigma_x + \sigma_x \eta_{D2} \{ \mathcal{K}_0, 2p_\xi \} - \sigma_y (\eta_{D1} + \eta_{D2} \{ 1, \mathcal{K}_0^2 \}) \right] \Big|_{p_\xi=0}$$

$$\{ 1, \mathcal{K}_0^2 \} = \frac{1}{2} (\mathcal{K}_0^2 + \mathcal{K}_0^2) = \mathcal{K}_0^2$$

$$\mathcal{H}_B = \eta_R \sigma_x - \sigma_y (\eta_{D1} + \eta_{D2} \mathcal{K}_0^2)$$

$$\mathcal{H}_C = \frac{1}{2!} \frac{\partial^2 \mathcal{H}}{\partial p_\xi^2} \Big|_{p_\xi=0} = \frac{1}{2} \left[ \sigma_0 + \sigma_x \eta_{D2} \{ \mathcal{K}_0, 2 \} \right] \Big|_{p_\xi=0}$$

$$\mathcal{H}_C = \frac{1}{2} \sigma_0 + \sigma_x \eta_{D2} \mathcal{K}_0$$

$$\begin{aligned}
\mathcal{H}_A &= \left[ \frac{1}{2} \mathcal{K}_0^2 + \frac{1}{2} \xi^2 \right] \sigma_0 + \frac{1}{2} \mathcal{B} (\cos \phi_B \sigma_x + \sin \phi_B \sigma_y) - \eta_R \sigma_y \mathcal{K}_0 + \eta_{D1} \sigma_x \mathcal{K}_0 \\
\mathcal{H}_B &= \eta_R \sigma_x - \sigma_y (\eta_{D1} + \eta_{D2} \mathcal{K}_0^2) \\
\mathcal{H}_C &= \frac{1}{2} \sigma_0 + \sigma_x \eta_{D2} \mathcal{K}_0
\end{aligned}$$

Up to now we haven't taken into account the exchange-correlation term and now we will mention about noncollinear local-spin density approximation.

### 5.3 Noncollinear Local-Spin Density Approximation

Above we have discussed for non-uniformly spin polarized systems. There are numerous spin-density functional calculations of the energy band structure of these systems. Common to all of these theories and calculations is the treatment of the magnetic moment as having only two directions, namely up and down. These moment arrangements are called collinear. The first work on disordered magnetic moments was investigated with the coherent potential approximation and the spin spirals was used that the magnetic moment was treated as a vector observable and noncollinear arrangements were admitted (Kübler, Höck, Sticht, & Williams, 1988). In the crystalline system the spin quantization axis is allowed to vary from site to site and there is no global spin quantization axis. In noncollinear magnets the orientation of the axes depends on some frame of reference, it is not arbitrary and a property of the ground state so it is an output quantity. Although the theory predicts well defined sets of directions for the spins, it doesn't couple the latter to the underlying crystal lattice, all that is important is their relative orientation. This changes when SO coupling is added the Hamiltonian.

When the magnetization direction changes in space then we can't use the approximation of constant magnetization direction. The problem we face to is construct a LDA for these systems. We follow an approach developed by Kübler and co-workers (Kübler et al, 1988). The underlying idea is to obtain a representation that locally diagonalizes the single particle density matrix by locally rotating the spin quantization axis. After constructing LDA the only requirement is exchange-correlation energy as

a function of spin-up and spin-down densities (or total density and polarization). The problem at Kohn-Sham Hamiltonian is unknown part exchange-correlation potential  $V_{\alpha\beta}^{xc}$ . An approximation definition in which the single-particle density matrix is diagonal with diagonal elements  $n_{\uparrow}$  and  $n_{\downarrow}$  was found by Kübler. The exchange-correlation potential can be written via chain rule

$$V_{\eta\eta'}^{xc} = \frac{\delta E_{xc}[n_{\uparrow}, n_{\downarrow}]}{\delta n_{\uparrow}} \frac{\partial n_{\uparrow}}{\partial \rho_{\eta\eta'}} + \frac{\delta E_{xc}[n_{\uparrow}, n_{\downarrow}]}{\delta n_{\downarrow}} \frac{\partial n_{\downarrow}}{\partial \rho_{\eta\eta'}} \quad (5.3.1)$$

We can find approximations for  $\delta E_{xc}/\delta n_{\sigma}$  via calculating exchange-correlation energy. The work is to calculate derivatives  $\partial n_{\uparrow}/\partial \rho_{\eta\eta'}$  and  $\partial n_{\downarrow}/\partial \rho_{\eta\eta'}$  which introduce the local spin rotation angles  $\theta(y)$  and  $\phi(y)$ . The angles give the orientation of the spin at point  $y$ . In the noncollinear case the density matrix is written in terms of particle and magnetization densities

$$\begin{aligned} \rho_{\eta\eta'}(y) &= \sum_n \frac{1}{2\pi} \int dk \varphi_{nk}^*(y, \eta) \varphi_{nk}(y, \eta') f_{\beta}(\epsilon_{nk}) \\ &\Rightarrow \begin{pmatrix} \rho_{\uparrow\uparrow} & \rho_{\uparrow\downarrow} \\ \rho_{\downarrow\uparrow} & \rho_{\downarrow\downarrow} \end{pmatrix} = \frac{1}{2} \begin{pmatrix} \rho + m_z & m_x + im_y \\ m_x - im_y & \rho - m_z \end{pmatrix} \end{aligned} \quad (5.3.2)$$

The density matrix ( $\rho_{\eta\eta'}$ ) is diagonalized via a local unitary transformation

$$U \rho U^{\dagger} = n \equiv \begin{pmatrix} n_{\uparrow} & 0 \\ 0 & n_{\downarrow} \end{pmatrix} \quad (5.3.3)$$

where the transformation is given as

$$U = \begin{pmatrix} e^{i\phi(y)/2} \cos \frac{\theta(y)}{2} & e^{-i\phi(y)/2} \sin \frac{\theta(y)}{2} \\ -e^{i\phi(y)/2} \sin \frac{\theta(y)}{2} & e^{-i\phi(y)/2} \cos \frac{\theta(y)}{2} \end{pmatrix} \quad (5.3.4)$$

The requirement that  $U$  diagonalizes  $\rho_{\eta\eta'}$  then the local rotation angles are

$$\tan \phi(y) = -\frac{m_y(y)}{m_x(y)}$$

and

$$\tan \theta(y) = \frac{\sqrt{m_x^2(y) + m_y^2(y)}}{m_z(y)}$$

From equation (5.3.3) diagonal densities  $n_\uparrow$  and  $n_\downarrow$  is calculated.

$$\begin{aligned} n_\uparrow &= \rho_{\uparrow\uparrow} \cos^2 \frac{\theta}{2} + \rho_{\uparrow\downarrow} e^{i\phi} \cos \frac{\theta}{2} \sin \frac{\theta}{2} + \rho_{\downarrow\uparrow} e^{-i\phi} \cos \frac{\theta}{2} \sin \frac{\theta}{2} + \rho_{\downarrow\downarrow} \sin^2 \frac{\theta}{2} \\ &= \frac{1}{2}(\rho + m_z \cos \theta) + \text{Re}\{\rho_{\uparrow\downarrow} e^{i\phi} \sin \theta\} \end{aligned} \quad (5.3.5)$$

$$\begin{aligned} n_\downarrow &= \rho_{\uparrow\uparrow} \sin^2 \frac{\theta}{2} - \rho_{\uparrow\downarrow} e^{i\phi} \cos \frac{\theta}{2} \sin \frac{\theta}{2} - \rho_{\downarrow\uparrow} e^{-i\phi} \cos \frac{\theta}{2} \sin \frac{\theta}{2} + \rho_{\downarrow\downarrow} \cos^2 \frac{\theta}{2} \\ &= \frac{1}{2}(\rho - m_z \cos \theta) - \text{Re}\{\rho_{\uparrow\downarrow} e^{i\phi} \sin \theta\} \end{aligned} \quad (5.3.6)$$

$\rho_{\eta\eta'}$  is diagonal and we know  $n_\uparrow$  and  $n_\downarrow$  at a point  $y$ , so that in the collinear LSDA we only need to know exchange-correlation energy as a function of total density and polarization. Undo this rotation the exchange-correlation potential can be calculated as

$$V_{\eta\eta'}^{xc} = \begin{pmatrix} v_0 + \Delta v \cos \theta & \Delta v e^{i\phi} \sin \theta \\ \Delta v e^{-i\phi} \sin \theta & v_0 - \Delta v \cos \theta \end{pmatrix} \quad (5.3.7)$$

where

$$\begin{pmatrix} v_\uparrow & 0 \\ 0 & v_\downarrow \end{pmatrix} \equiv \begin{pmatrix} \delta E_{xc}[n_\uparrow, n_\downarrow] / \delta n_\uparrow & 0 \\ 0 & \delta E_{xc}[n_\uparrow, n_\downarrow] / \delta n_\downarrow \end{pmatrix} \quad (5.3.8)$$

and  $v \equiv (v_\uparrow + v_\downarrow)/2$  and  $\Delta v \equiv (v_\uparrow - v_\downarrow)/2$ . Thus the exchange-correlation potential matrix was written in terms of spinor orbitals and LSDA energy density functional. In the LDA the exchange-correlation energy can be written as the function of polarization and filling factor instead of density. The relation between density and filling factor is  $v(y) = 2\pi b_0^2 n(y)$  and we can write exchange-correlation energy

$$E_{xc} = \int dy n(y) \epsilon_{xc}[v(y), \zeta(y)] \quad (5.3.9)$$

where  $\epsilon_{xc}$  is the exchange-correlation energy per particle in an infinite, homogenous system of filling factor  $v$  and polarization  $\zeta$ . In this new formulation polarization can be redescribed function of filling factor  $\zeta = (v_\uparrow - v_\downarrow)/v$ . The new definition of  $v_\uparrow$

and  $v_{\downarrow}$  (Heinonen, Kinaret, & Johnson, 1999).

$$\begin{aligned} v_{\uparrow} &= \left[ \frac{\partial}{\partial v} + \frac{1}{v}(1 - \zeta) \frac{\partial}{\partial \zeta} \right] [v \epsilon_{xc}(v, \zeta)] \\ v_{\downarrow} &= \left[ \frac{\partial}{\partial v} - \frac{1}{v}(1 + \zeta) \frac{\partial}{\partial \zeta} \right] [v \epsilon_{xc}(v, \zeta)] \end{aligned} \quad (5.3.10)$$

In this work the exchange-correlation energy functional was taken from the work of Attaccalite and coworkers (Attaccalite et al, 2002; 2003).

## CHAPTER SIX

### RESULTS

In this study, we have investigated the electronic structure of quantum wires obtained of confining the GaAs heterostructure. The bulk parameters  $g^* = -0.44$ ,  $m^* = 0.067$  and dielectric constant  $\epsilon = 12.4$  have been used. We have defined the SO regime with the ratio of the strength of SO interaction to confinement potential.

$$\Delta_{R,D} = \frac{m^* \lambda_{R,D}^2}{2\hbar^3 \omega_0}$$

For strong SO regime  $\Delta_R = 0.093$ ,  $\Delta_D = 0.37$  values have been used and for weak SO regime  $\Delta_R = 0.0037$ ,  $\Delta_D = 0.015$  have been used (Zhang et al, 2006). For GaAs/AlGaAs SO coupling constants are experimentally in order of  $10^{-11}$  eVm (Miller et al, 2003; Könemann, Haug, Maude, Fal'ko, & Altshuler, 2005). We have given the results of strong and weak SO regime in this study.

We investigated some cases for different strength of SO interaction and in the presence or absence of magnetic field. A comprehensive study as a function of parameter space can be carried out but we have restricted our work for some examples. When applied magnetic field is different from zero we have set it to 20 T and have considered three orientations of it, namely,  $\phi_B = 0$ ,  $\phi_B = \pi/4$  and  $\phi_B = \pi/2$ . The harmonic oscillator length  $b_0 = \sqrt{\hbar/m^* \omega_0}$  is used to identify the results and the energies are scaled in  $\hbar\omega_0$  units. The value of  $\hbar\omega_0$  is set to 4 meV which is a typical energy value for GaAs system.

We studied the exchange-correlation effect on the energy subband structure in some cases which involve in-plane magnetic field and different strengths of SO interaction. Systematizing the effect of the exchange-correlation energy is difficult because it depends on the other parameters which are used to characterize the QW, such as linear density  $\rho_{1D}$ , SO coupling constants  $\lambda_{R,D}$  and  $\phi_B$  the orientation of magnetic field.

## 6.1 The Effect of Spin-Orbit Interaction and Magnetic Field

In the first part of results we present the effects of SO interaction and magnetic field on the subband structure when exchange-correlation energy is not taken into account.

We firstly wanted to identify the effect of SO interaction on the energy subbands

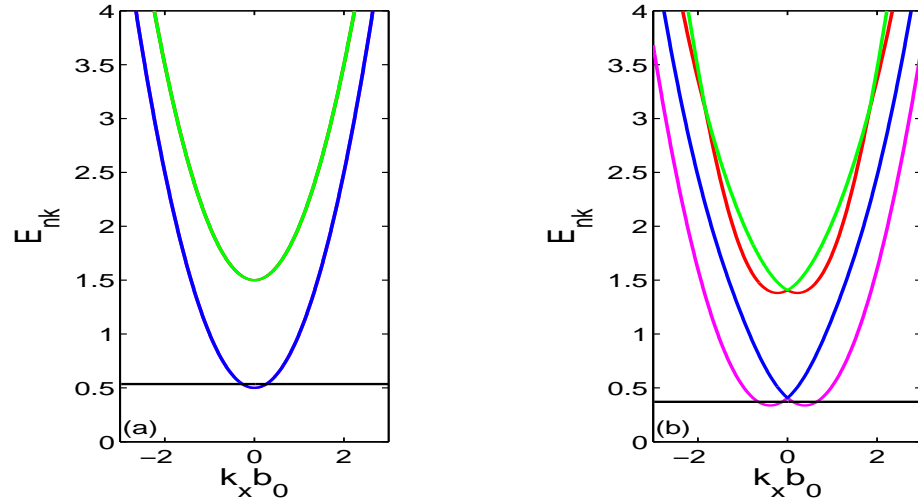


Figure 6.1 Single electron energies (in  $\hbar\omega_0$  units) for  $\rho_{1D}b_0 = 0.17$  as a function of  $k_x b_0$ . (a) corresponds to  $\Delta_R = 0$ ,  $\Delta_D = 0$ ,  $B = 0$  and (b)  $\Delta_R = 0.093$ ,  $\Delta_D = 0$ ,  $B = 0$

in the absence of an external magnetic field. In Figure 6.1(a) energy subbands are graphed in the absence of magnetic field and SO interaction for a low density such as  $\rho_{1D}b_0 = 0.17$ . Each subband shows twofold degenerate parabola for the two different spin orientations. The energy subbands are spin-up and down degenerate for all  $k_x$  values. We present the effect of including SO interaction to the degeneracy in the Figure 6.1(b). We addressed the Rashba SO interaction in the Figure 6.1(b) but we have observed that Rashba and Dresselhaus SO interactions have same effect on the energy dispersion which shows same behaviors for the same characteristic SO interaction. For in the presence of a weak Rashba (or Dresselhaus) SO interaction, namely  $\Delta_R = 0.093$ , the degenerate energy subbands split into two laterally displaced parabolas except the point at  $k_x = 0$  (Zhang et al, 2009). Rashba SO interaction breaks down the degeneracy. In this Figure 6.1(b) we don't consider the coupling between different subbands.

In Figure 6.1(b), it is seen that the weak Rashba SO interaction lifts the degeneracy for  $k$  values except  $k_x = 0$ . In Figure 6.2(a) for the same value of Rashba SO inter-

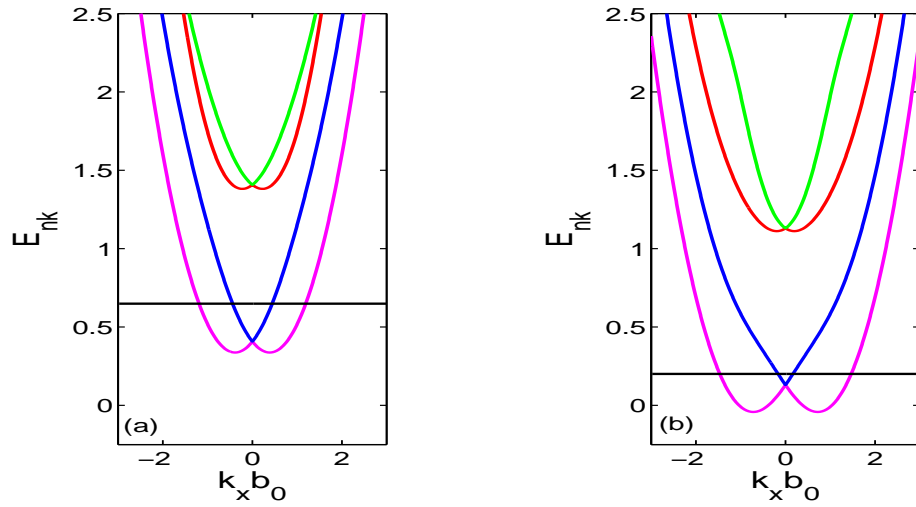


Figure 6.2 Single electron energies (in  $\hbar\omega_0$  units) for  $\rho_{1D}b_0 = 0.52$  as a function of  $k_x b_0$ . (a)  $\Delta_R = 0.093$ ,  $\Delta_D = 0$ ,  $B = 0$  and (b)  $\Delta_R = 0.037$ ,  $\Delta_D = 0$ ,  $B = 0$

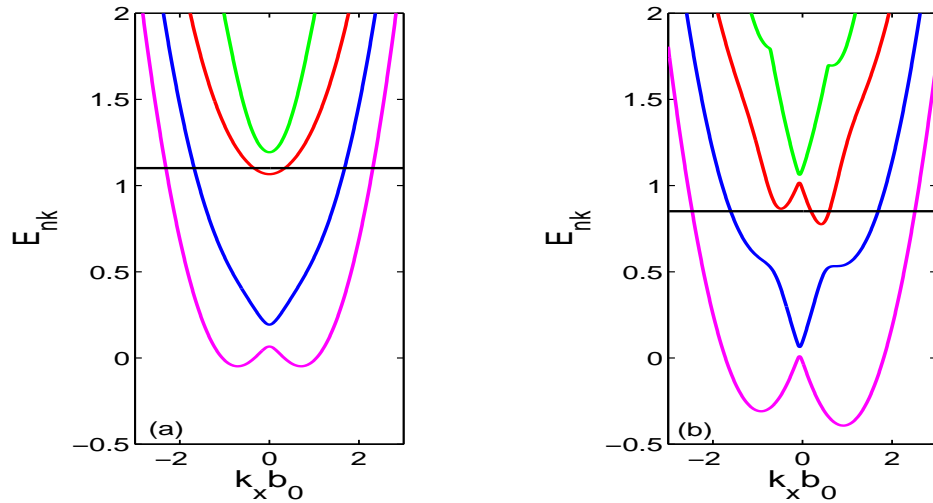


Figure 6.3 Single electron energies (in  $\hbar\omega_0$  units) for  $\rho_{1D}b_0 = 1.38$  as a function of  $k_x b_0$ . (a)  $\Delta_R = 0$ ,  $\Delta_D = 0.37$ ,  $B = 20$  T,  $\phi_B = \pi/2$  and (b)  $\Delta_R = 0.093$ ,  $\Delta_D = 0.37$ ,  $B = 20$  T,  $\phi_B = \pi/2$

action,  $\Delta_R = 0.093$ , but a different value of density  $\rho_{1D}b_0 = 0.52$ , weak anticrossings occur between different spin orientation within the same subband at low  $k_x$  values. At higher values of  $k_x$  weak coupling occurs between different spin orientation and different subbands. The  $k$ -splitting which arises from the linear terms in momentum ( $\mathbf{p}$ ) of  $\mathcal{H}_{SO}$  increases in the presence of strong Rashba SO interaction such as  $\Delta_R = 0.037$ . The energy subbands are still degenerate at point  $k_x = 0$ . The different spin orientation within each subband leads to anticrossing at the large values of  $k_x$ . The crossings which



are seen in the presence of weak Rashba SO interaction vanish when strong SO interaction, of which values is  $\Delta_R = 0.037$ , is considered as seen in Figure 6.2(b) (Knobbe, & Schapers, 2005; Serra et al, 2005).

In Figure 6.3(a) we show the variation of energy in the presence of an applied magnetic field which indicate y-direction, i.e.,  $\phi_B = \pi/2$  and set to 20 T and also for a high density value  $\rho_{1D}b_0 = 1.38$ . In this case, strong Dresselhaus SO interaction, namely,  $\Delta_D = 0.37$ , lifts the the spin degeneracy of subbands for all k values and lower subbands develops a camelback shape. We see a symmetric double minimum structure in the first subband. By the inclusion of weak Rashba SO interaction characterized by  $\Delta_R = 0.093$ , the camelback shape disappears Figure 6.3(b). The symmetric double minimum structure in the absence of Rashba SO interaction turns into the asymmetric shape when Rashba SO interaction is taken into account. These k-asymmetries appear for almost all bands. Near  $k_x = 0$  conspicuous subband gap and local extrema is seen. In the even subbands we observe anomalous steps as reported by Zhang and co-workers (Zhang et al, 2006).

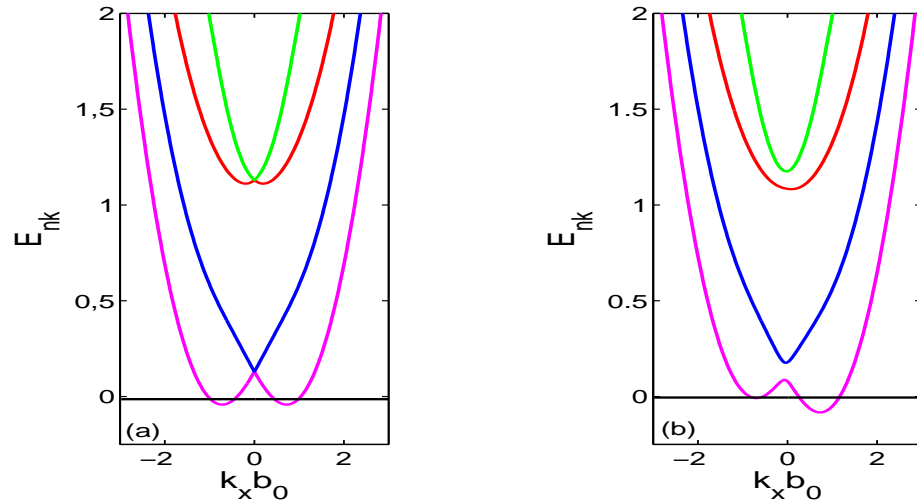


Figure 6.4 Single electron energies (in  $\hbar\omega_0$  units) for  $\rho_{1D}b_0 = 0.17$  as a function of  $k_x b_0$ . (a)  $\Delta_R = 0.37$ ,  $\Delta_D = 0$ ,  $B = 0$  and (b)  $\Delta_R = 0.37$ ,  $\Delta_D = 0$ ,  $B = 20$ ,  $\phi_B = \pi/4$

The effect of magnetic field on the subband structure is important for identifying the beating pattern in the magnetoresistance so we want the understand the effect of an external applied magnetic field. Figure 6.4 shows the relation between magnetic field and energy subband for low density  $\rho_{1D}b_0 = 0.17$  and in the presence of strong Rashba

SO interaction, namely  $\Delta_R = 0.37$ . When there is no external magnetic field the energy subbands show degeneracy at  $k_x = 0$  as seen in Figure 6.4(a). When an external magnetic field is applied the separation between subbands, namely k-splitting, becomes larger and the previous spin degeneracy at point  $k_x = 0$  is lifted. In the first subband asymmetry is observed. The magnetic field and SO interaction cause a complex energy spectrum and the gaps between different subbands vary for different  $k$  values at a constant magnetic field. It leads to a characteristic beating pattern in the magnetoresistance (Zhang et al,2006; Pramanik, Bandyopadhyay, & Cahay, 2007).

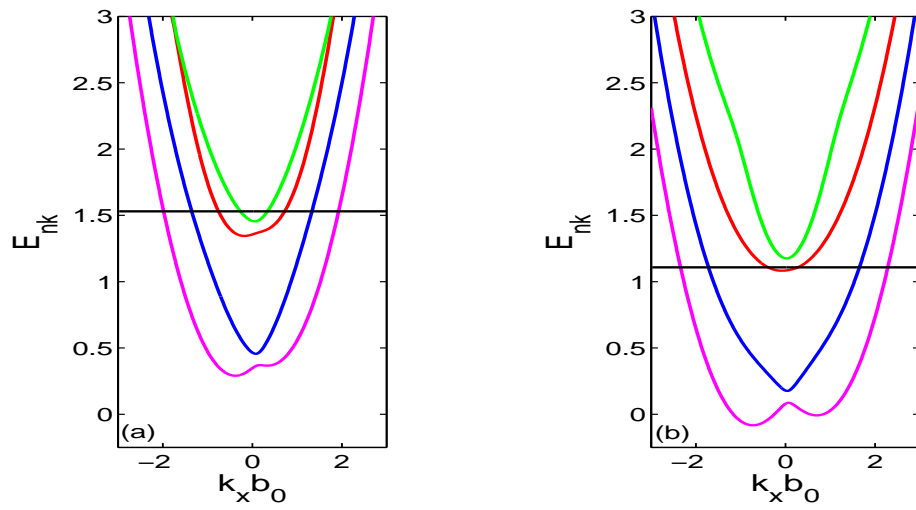


Figure 6.5 Single electron energies (in  $\hbar\omega_0$  units) for  $\rho_{1D}b_0 = 1.38$  as a function of  $k_x b_0$ . (a)  $\Delta_R = 0$ ,  $\Delta_D = 0.093$ ,  $B = 20$  T,  $\phi_B = \pi/4$  and (b)  $\Delta_R = 0$ ,  $\Delta_D = 0.37$ ,  $B = 20$  T,  $\phi_B = \pi/4$

In this Figure 6.5 we consider the Dresselhaus SO effect on the energy dispersion in the presence of strong magnetic field which orientates with the angle  $\phi_B = \pi/4$ . When only Dresselhaus SO interaction, which corresponds to weak interaction with the value of  $\Delta_D = 0.093$ , is considered the energy subbands are degenerate at  $k_x = 0$  but applying an external magnetic field the degeneracy of the two different spin orientations of each subband is lifted. For the weak Dresselhaus SO interaction the separation between the neighbour energy subbands decreases with increasing  $n$ . For the higher values of  $n$  the k-splitting branches have different shapes and they cross each other, the crossings are observed as seen in Figure 6.5(a). Including strong Dresselhaus SO interaction, namely  $\Delta_D = 0.37$ , the lower branches of each subband constitute a camelback shape in the environs of  $k_x = 0$ . The crossings caused by the weak SO interaction is lifted in the presence of strong Dresselhaus SO interaction as shown in Figure 6.5(b).

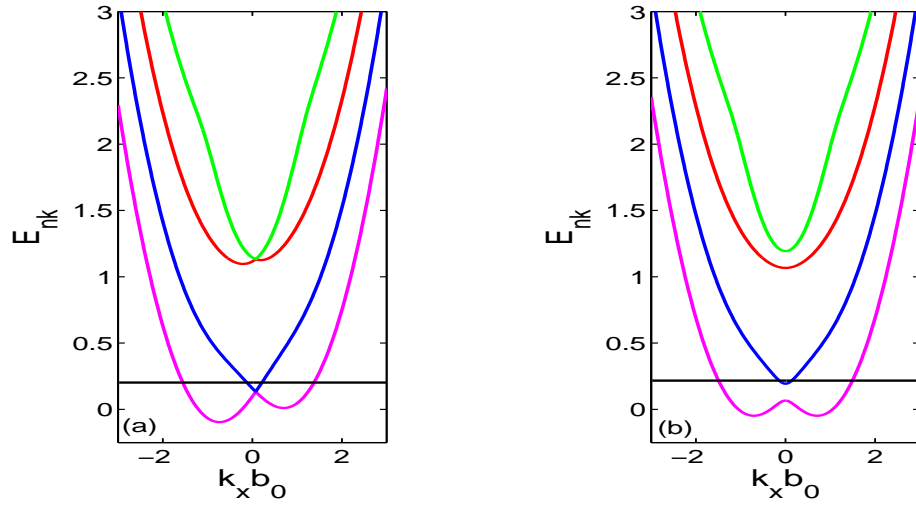


Figure 6.6 Single electron energies (in  $\hbar\omega_0$  units) for  $\rho_{1D}b_0 = 0.52$  as a function of  $k_x b_0$ . (a)  $\Delta_R = 0$ ,  $\Delta_D = 0.37$ ,  $B = 20$  T,  $\phi_B = 0$  and (b)  $\Delta_R = 0$ ,  $\Delta_D = 0.37$ ,  $B = 20$  T,  $\phi_B = \pi/2$

We want to identify the dependence of the energy subbands on the orientation of the magnetic field. Therefore in Figure 6.6 we plot the energy subband structure for the parameters  $\rho_{1D}b_0 = 0.52$ ,  $\Delta_R = 0$ ,  $\Delta_D = 0.37$  and  $B = 20$  T. Figure 6.6(a) corresponds to the case of  $B = 0$  and strong Dresselhaus SO interaction the energy subbands are degenerate at  $k_x = 0$ . Applying an external magnetic field along x-direction doesn't lift this degeneracy. It induces k-asymmetries. When the magnetic field is applied along the y-direction the degeneracy caused by the two different spin orientations at point  $k_x = 0$  is lifted, the k-splitting increases as seen in Figure 6.6(b). The k-asymmetries vanish and the a symmetric double minimum structure occurs in the first subband by applying magnetic field. In contrast to zero magnetic field anticrossing of subbands doesn't appear.

Now we compare the energy subbands for a strong magnetic field and two types of strong SO interaction. Rashba and Dresselhaus SO interactions present simultaneously but in different strengths, namely we exchange their values. When Rashba SO interaction is stronger in Figure 6.7(a) with the interaction strengths are  $\Delta_R = 0.37$ ,  $\Delta_D = 0.093$ , in Figure 6.7(b) the interactions are changed and Dresselhaus SO interaction is dominant, namely  $\Delta_R = 0.093$ ,  $\Delta_D = 0.37$ . For strong Rashba SO interaction k-asymmetries occur in the odd subbands. In the even subbands anomalous steps occur which arise from the combined effect of SO and magnetic field B as seen in Figure

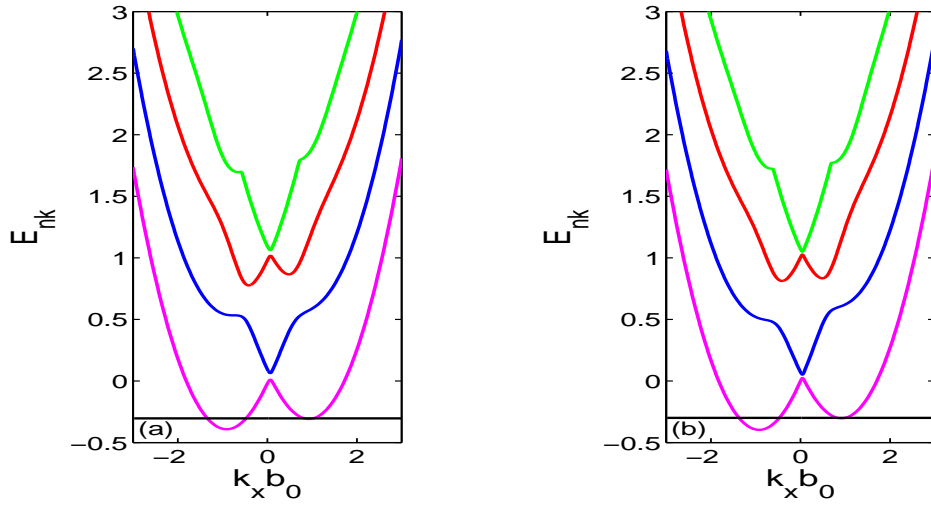


Figure 6.7 Single electron energies (in  $\hbar\omega_0$  units) for  $\rho_{1D}b_0 = 0.17$  as a function of  $k_x b_0$ . (a)  $\Delta_R = 0.37$ ,  $\Delta_D = 0.093$ ,  $B = 20$  T,  $\phi_B = 0$  and (b)  $\Delta_R = 0.093$ ,  $\Delta_D = 0.37$ ,  $B = 20$  T,  $\phi_B = 0$

6.7(a). And Figure 6.7(b) shows the energy dispersion for strong Dresselhaus SO interaction. The symmetric structure in the third subband turns into asymmetric shape. The plateaus also occur in the even subbands (Zhang et al ,2006; Malet et al, 2007; Zhang et al, 2009) .

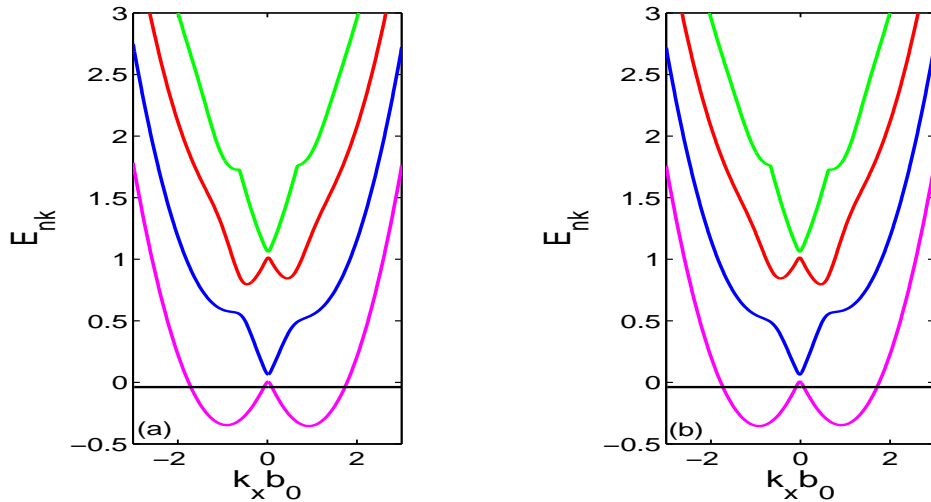


Figure 6.8 Single electron energies (in  $\hbar\omega_0$  units) for  $\rho_{1D}b_0 = 0.52$  as a function of  $k_x b_0$ . (a)  $\Delta_R = 0.37$ ,  $\Delta_D = 0.093$ ,  $B = 20$  T,  $\phi_B = \pi/4$  and (b)  $\Delta_R = 0.093$ ,  $\Delta_D = 0.37$ ,  $B = 20$  T,  $\phi_B = \pi/4$

In Figure 6.8 we consider a different orientation  $\phi_B = \pi/4$  of magnetic field in the presence of strong SO interaction. Figure 6.8(a) and Figure 6.8(b) corresponds the different strengths of Rashba and Dresselhaus SO interactions. It is seen that in both

strong SO regime k-asymmetries are induced for odd subbands  $n > 1$ . In the ground state there is symmetric double minimum. For the different strength of SO interaction subbands show inversion symmetry to  $k_x = 0$ .

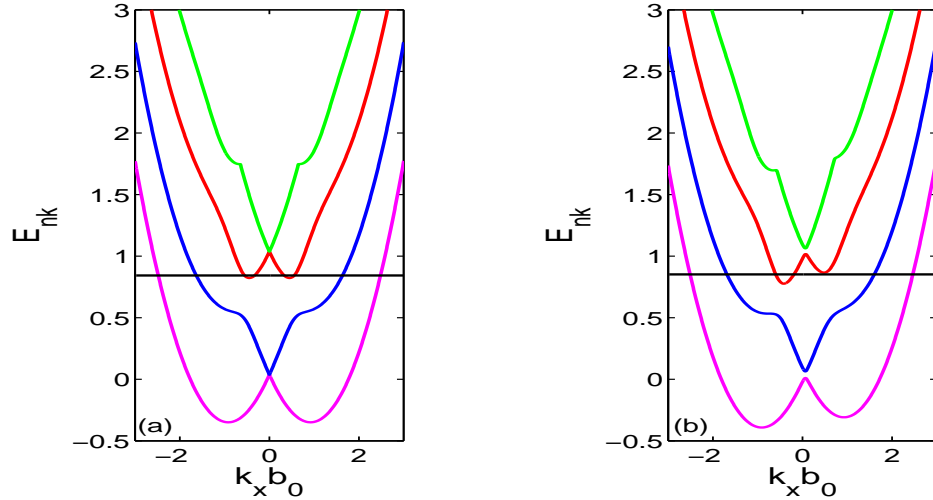


Figure 6.9 Single electron energies (in  $\hbar\omega_0$  units) for  $\rho_{1D}b_0 = 1.38$  as a function of  $k_x b_0$ . (a)  $\Delta_R = 0.37$ ,  $\Delta_D = 0.093$ ,  $B = 0$  and (b)  $\Delta_R = 0.37$ ,  $\Delta_D = 0.093$ ,  $B = 20$  T,  $\phi_B = 0$

In Figure 6.9, we want to identify the effect of magnetic field for the strong regime which is characterized by  $\Delta_R = 0.37$ ,  $\Delta_D = 0.093$  in the high density limit. When  $B = 0$ , which is shown in Figure 6.9(a), the energy subbands are degenerate at  $k_x = 0$ . Symmetric weak local minimum occurs for the even subbands. In Figure 6.9(b), by applying an external magnetic field this degeneracy is lifted. The magnetic field gives rise to k-asymmetries and subband splitting. In the presence of an external magnetic field and strong SO interaction, we observe conspicuous subband gaps and the so-called anomalous plateaus.

## 6.2 The Effects of Exchange-Correlation Energy

After having learned the effects of SO interaction and magnetic field on the energy dispersion, we now search the effect of exchange-correlation energy. From Figure 6.10 to Figure 6.17, with solid lines we show the energy subbands without inclusion of exchange-correlation effect while the dashed lines correspond to  $V^{xc} \neq 0$ . Figure 6.10, presented for the low density limit such as  $\rho_{1D}b_0 = 0.17$ , shows that the weak Rashba

SO interaction and the magnetic field induce asymmetry in the odd bands. The effect of the exchange-correlation energy is to break down this asymmetry and to transform the subbands like parabola shape as seen in Figure 6.10(a). In the presence of strong Rashba SO interaction the subband structure is graphed in Figure 6.10(b). It is seen that the asymmetry in the ground state remains when  $V^{xc}$  is taken into account.

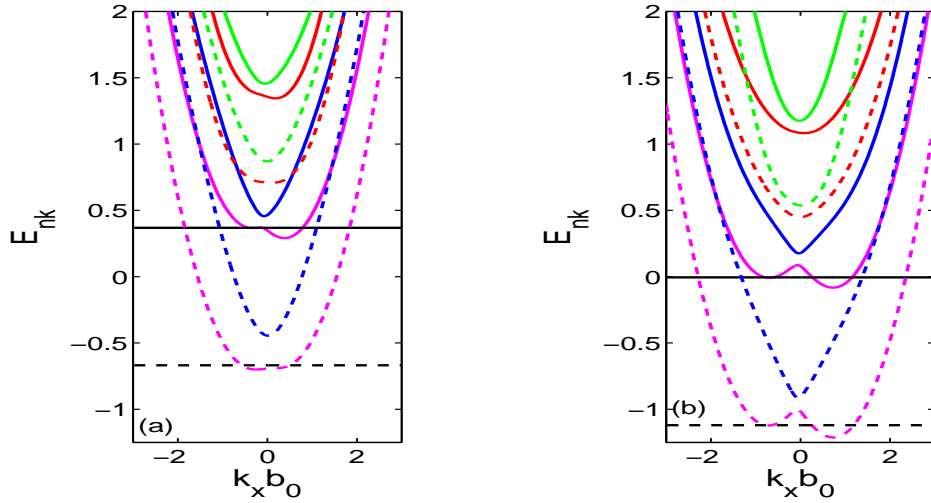


Figure 6.10 Single electron energies (in  $\hbar\omega_0$  units) for  $\rho_{1D}b_0 = 0.17$  as a function of  $k_x b_0$ . (a)  $\Delta_R = 0.093$ ,  $\Delta_D = 0$ ,  $B = 20$  T,  $\phi_B = \pi/4$  and (b)  $\Delta_R = 0.37$ ,  $\Delta_D = 0$ ,  $B = 20$  T,  $\phi_B = \pi/4$

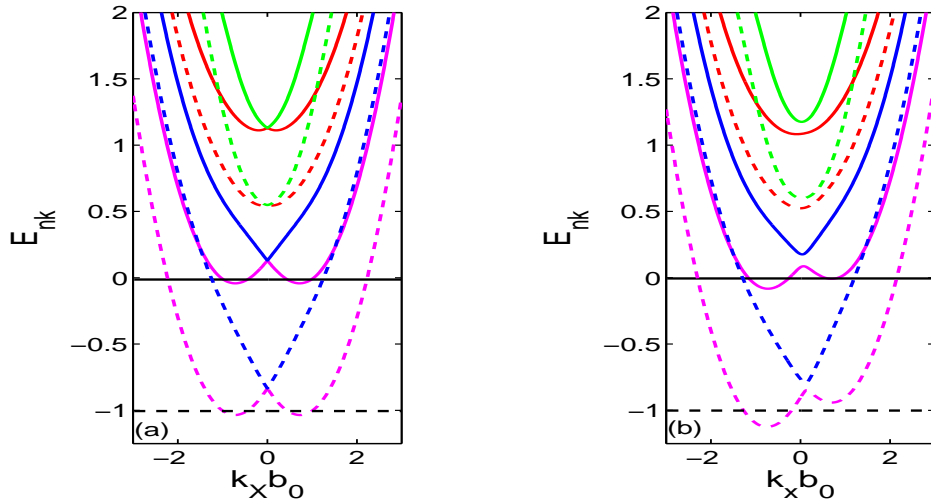


Figure 6.11 Single electron energies (in  $\hbar\omega_0$  units) for  $\rho_{1D}b_0 = 0.17$  as a function of  $k_x b_0$ . (a)  $\Delta_R = 0$ ,  $\Delta_D = 0.37$ ,  $B = 0$  and (b)  $\Delta_R = 0$ ,  $\Delta_D = 0.37$ ,  $B = 20$  T,  $\phi_B = \pi/4$

Figure 6.11 shows the exchange-correlation effect in the presence of strong Dresselhaus SO interaction characterized by  $\Delta_D = 0.37$ . For a strong Dresselhaus SO interaction when  $B = 0$  the subbands show degeneracy at point  $k_x = 0$ . When  $V^{xc}$  is considered

the energy subbands shift to lower energy values as seen in Figure 6.11(a). Applying an external magnetic field but remaining the strength of SO interaction, the degeneracy lifts and transforms the double minimum shape to an asymmetry in the ground state. By adding the  $V^{xc}$  this asymmetry increases on the other hand the k-splitting decreases. When  $B \neq 0$ ,  $V^{xc}$  seems to change the value of  $\phi_B$  or increase the intensity of B. This case is graphed in Figure 6.11(b).

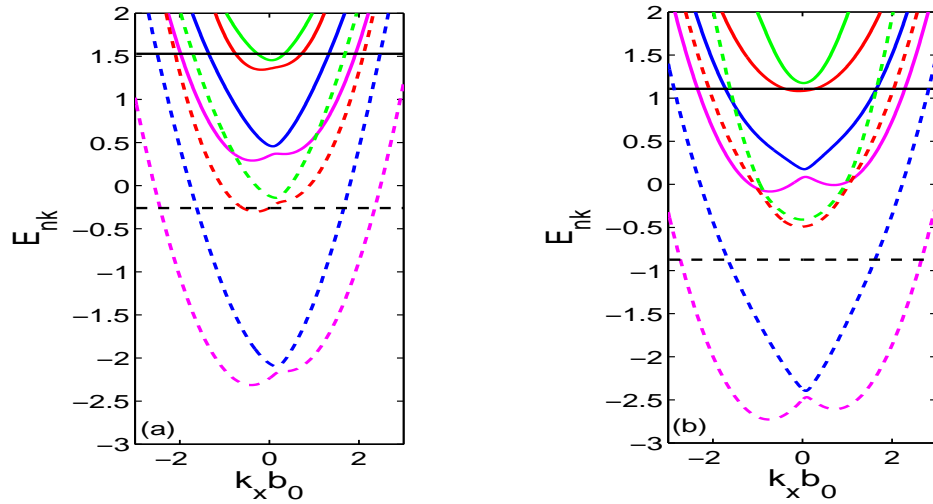


Figure 6.12 Single electron energies (in  $\hbar\omega_0$  units) for  $\rho_{1D}b_0 = 1.38$  as a function of  $k_x b_0$ . (a)  $\Delta_R = 0$ ,  $\Delta_D = 0.093$ ,  $B = 20$  T,  $\phi_B = \pi/4$  and (b)  $\Delta_R = 0$ ,  $\Delta_D = 0.37$ ,  $B = 20$  T,  $\phi_B = \pi/4$

Figure 6.12 shows the result corresponding to a high density  $\rho_{1D}b_0 = 1.38$  for an applied magnetic field of 20 T and  $\phi_B = \pi/4$  in the different strengths of Dresselhaus SO interaction. Weak Dresselhaus SO interaction induces weak k-asymmetries for odd bands. Exchange-correlation effects predominantly appears on these asymmetries, it increases the asymmetry shapes in the odd subbands and shifts all of the subbands to the lower energy values as seen in Figure 6.12(a). The effect of exchange-correlation energy in the strong Dresselhaus regime is shown in Figure 6.12(b). Including  $V^{xc}$  doesn't change the k-asymmetries but it decreases the k-splitting especially for higher subbands.

Figure 6.13 shows the energy subband structure with these parameters  $\rho_{1D}b_0 = 0.17$ ,  $\Delta_R = 0.093$ ,  $B = 20$  T,  $\phi_B = \pi/4$ . It can be seen in Figure 6.13(a), for a weak Rashba SO interaction, inclusion of the exchange-correlation energy changes the asymmetries, it transforms these structures into a parabola like subbands. A strong SO

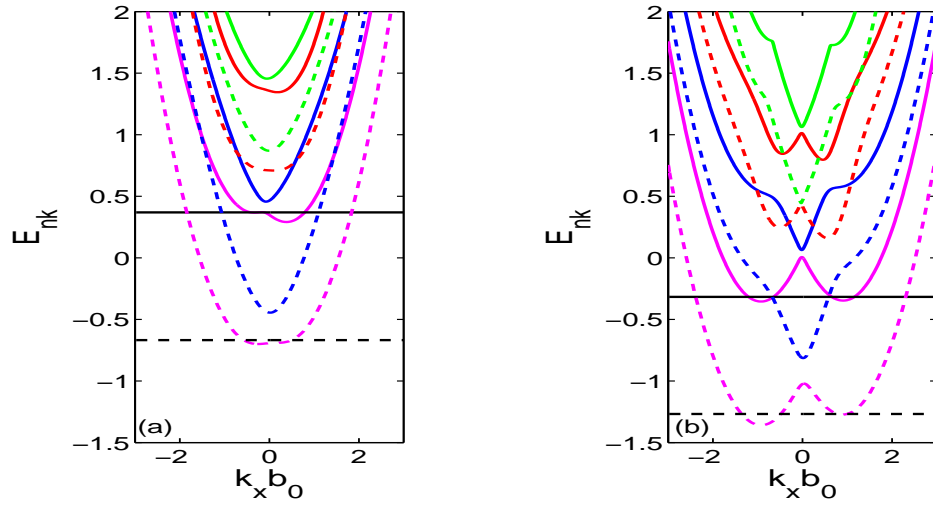


Figure 6.13 Single electron energies (in  $\hbar\omega_0$  units) for  $\rho_{1D}b_0 = 0.17$  as a function of  $k_x b_0$ . (a)  $\Delta_R = 0.093$ ,  $\Delta_D = 0$ ,  $B = 20$  T,  $\phi_B = \pi/4$  and (b)  $\Delta_R = 0.093$ ,  $\Delta_D = 0.37$ ,  $B = 20$  T,  $\phi_B = \pi/4$

regime which includes both Rashba and Dresselhaus, induces anomalous plateaus in the even subbands. The exchange-correlation energy smooths these structures and transforms the symmetric shapes to asymmetric shapes in the odd bands. We see this situation in Figure 6.13(b).

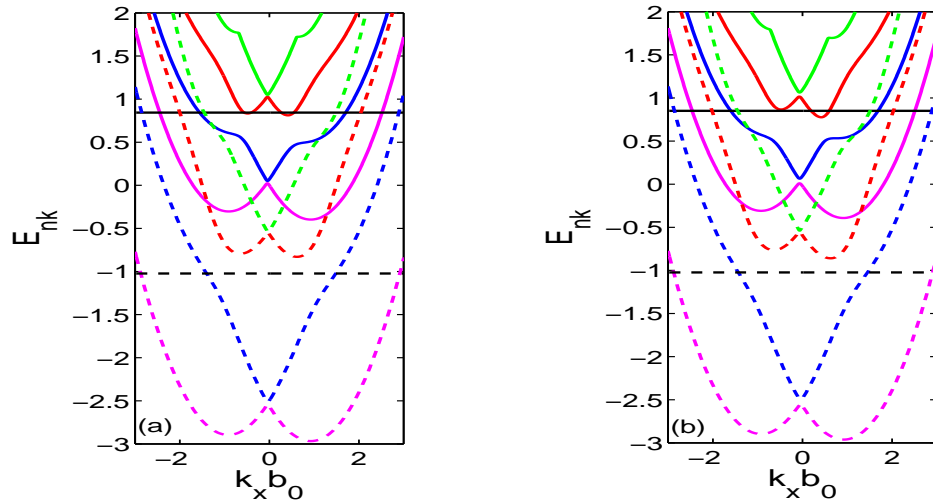


Figure 6.14 Single electron energies (in  $\hbar\omega_0$  units) for  $\rho_{1D}b_0 = 1.38$  as a function of  $k_x b_0$ . (a)  $\Delta_R = 0.37$ ,  $\Delta_D = 0.093$ ,  $B = 20$  T,  $\phi_B = \pi/2$  and (b)  $\Delta_R = 0.093$ ,  $\Delta_D = 0.37$ ,  $B = 20$  T,  $\phi_B = \pi/2$

When both SO interactions have taken into account we can also observe the effect of exchange-correlation, as seen Figure 6.14. We study the the exchange-correlation effects for strong SO regime different values of Rashba and Dresselhaus SO interaction



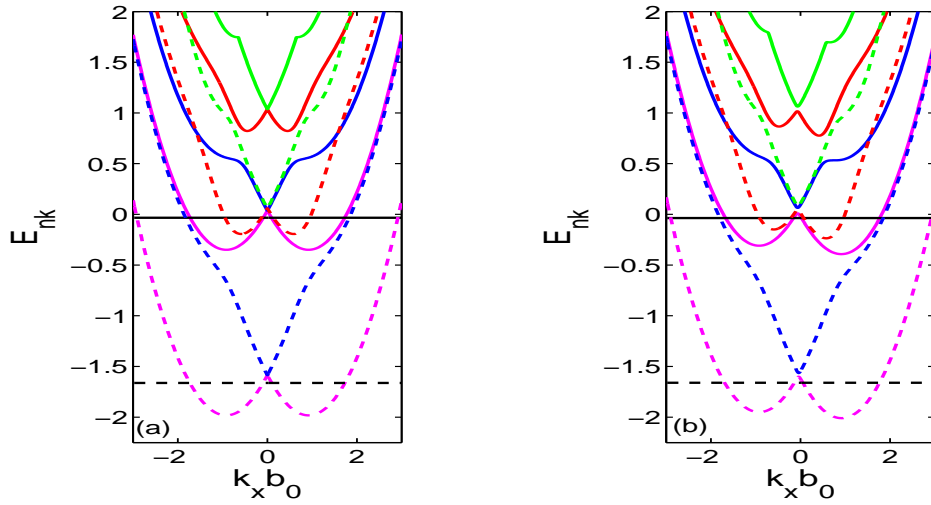


Figure 6.15 Single electron energies (in  $\hbar\omega_0$  units) for  $\rho_{1D}b_0 = 0.52$  as a function of  $k_x b_0$ . (a)  $\Delta_R = 0.093$ ,  $\Delta_D = 0.37$ ,  $B = 0$  and (b)  $\Delta_R = 0.093$ ,  $\Delta_D = 0.37$ ,  $B = 20$  T,  $\phi_B = \pi/2$

and in the presence of magnetic fields which indicate  $y$ -direction, i.e.,  $\phi_B = \pi/2$ . We can see subband gaps in both graphs and for four cases. The interaction between SO and magnetic field causes anomalous plateaus. It can be seen that the inclusion of  $V^{xc}$  washes out these plateaus. We can obtain same results with Malet (Malet et al, 2007) for Figure 6.14 (b).

For strong regime characterized by  $\Delta_R = 0.093$  and  $\Delta_D = 0.37$ , the exchange-correlation effect is studied for  $B = 0$  and  $B = 20$  T and  $\phi_B = \pi/2$  which is shown in Figure 6.15. When  $B \neq 0$ ,  $\varepsilon_{xc}$  seems to change the value of  $\phi_B$  or increase the intensity of  $B$ . Including the  $V^{xc}$  the local maximums at even subbands are smoothed.

We want to identify the dependence of the energy subbands on density. Therefore in Figure 6.16 we plot the energy subband structure for the parameters  $\Delta_R = 0.093$ ,  $\Delta_D = 0.37$ ,  $B = 20$  T,  $\phi_B = \pi/4$  and two values of density. Figure 6.16(a) corresponds to low density  $\rho_{1D}b_0 = 0.17$  and the high density such as  $\rho_{1D}b_0 = 1.38$  is shown in Figure 6.16(b). Inclusion of exchange-correlation energy changes the symmetry in the odd bands, it induces asymmetries. We can see that the  $\varepsilon_{xc}$  smooths the local maximums at even subbands. When the  $k$ -splitting increases for lower subbands, at higher value of energy values  $k_x = 0$  degeneracy occurs. The energy dispersion shows similar characteristics for different densities.

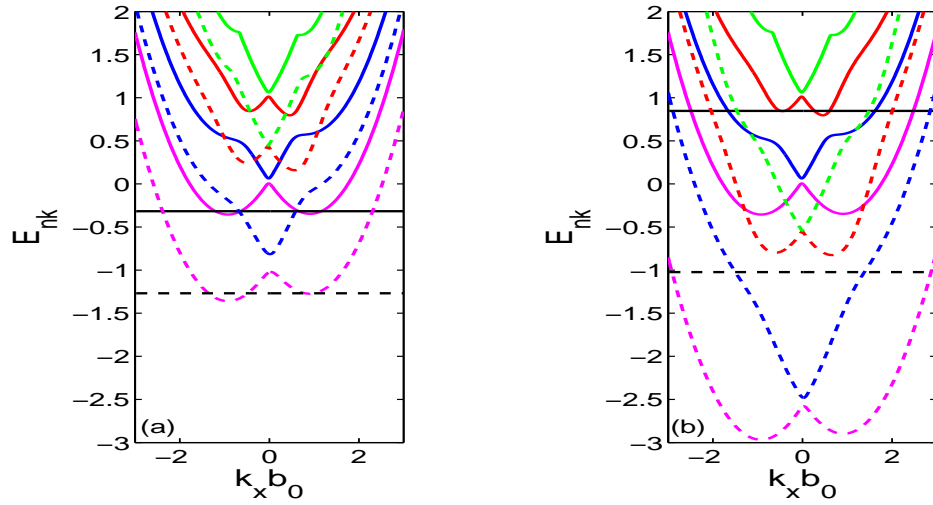


Figure 6.16 Single electron energies (in  $\hbar\omega_0$  units) as a function of  $k_x b_0$ . (a)  $\Delta_R = 0.093$ ,  $\Delta_D = 0.37$ ,  $B = 20$  T,  $\phi_B = \pi/4$ ,  $\rho_{1D} b_0 = 0.17$  and (b)  $\Delta_R = 0.093$ ,  $\Delta_D = 0.37$ ,  $B = 20$  T,  $\phi_B = \pi/4$ ,  $\rho_{1D} b_0 = 1.38$

We have obtained same results with Malet (Malet et al, 2007) at high values of density but in the low density limit our results differs from each other. This discrepancy can be due to different choices for the exchange-correlation energies. We have used Attaccalite (Attaccalite et al, 2002) parametrization for exchange-correlation energy whereas they used von Barth and Hedin prescription (von Barth & Hedin, 1972). von Barth and Hedin calculate exchange-correlation energy functional for fully polarized and nonpolarized two-dimensional electron gas and interpolate energy functional between these two regimes. Attaccalite parametrization doesn't require any interpolation so the energy functional. According to Malet and co-workers (Malet et al, 2007) using the improved energy functional would not make an substantial changes in the results, but we have seen that especially in the low density limits the results are different. The effects of improved  $\epsilon_{xc}$  can be clearly seen in the figures. It has been observed that  $V^{xc}$  tends to increase the effects of magnetic fields and especially at low density limits it act as if an applied magnetic field. In some situations, when  $B = 0$  involving the exchange-correlation the subband structure seems same as  $V^{xc} = 0$  but as if a magnetic field is applied. The magnetization which consists as a result of the spontaneous symmetry breaking can be made by the exchange-correlation energy. In the presence of an external magnetic field  $V^{xc}$  may act as if an additional magnetic field and it enhance the value of B or contributes to create an in-plane magnetic field which heads to different direction from existing magnetic field.

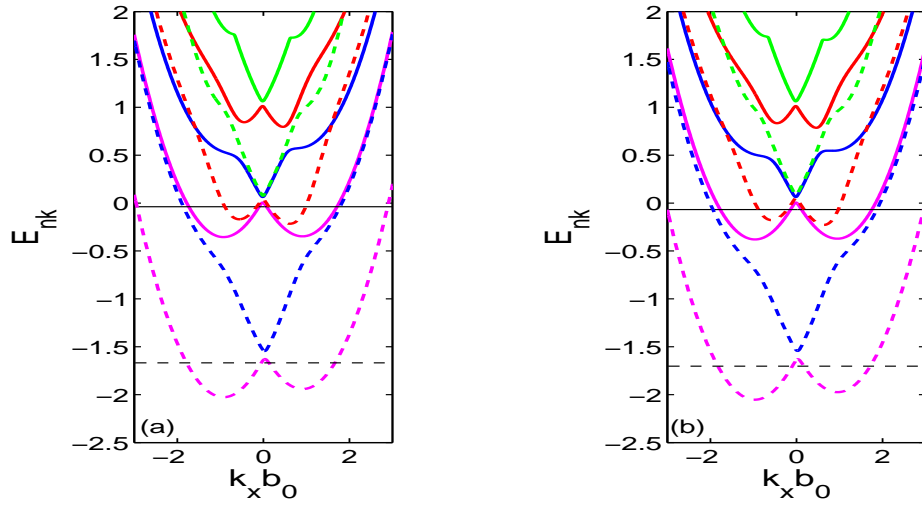


Figure 6.17 Single electron energies (in  $\hbar\omega_0$  units) as a function of  $k_x b_0$ .  $\Delta_R = 0.093$ ,  $\Delta_D = 0.37$ ,  $B = 20$  T,  $\phi_B = \pi/4$ ,  $\rho_{1D} b_0 = 0.52$  (a) without cubic Dresselhaus term (b) with cubic Dresselhaus terms

We also have investigated the contribution of the cubic Dresselhaus SO interaction. In Figure 6.17, the left panel (a) corresponds the energy dispersion with the off-neglected cubic Dresselhaus terms. In the right panel (b) we can see the contribution of cubic terms. The cubic Dresselhaus SO coupling constant is related to linear Dresselhaus SO coupling constant and the relation between them is  $\beta_D = \hbar\omega_o\gamma_D\langle k_z^2 \rangle$  (Studer et al, 2010) and  $\langle k_z^2 \rangle \alpha(\pi/L)^2$ . We have obtained energy dispersion for a moderate value of  $k_z^2$ . It has been experimentally observed that cubic Dresselhaus SO interactions become important for the high densities, weak electron confinement and lower values of  $\gamma_D$  (Studer et al, 2010) and it plays a strong and previously ignored role in observed transport properties (Krich & Bertrand, 2007). We have observed in our study that the contribution of the cubic Dresselhaus term gives rise to a small shift in energy subbands which can be due to moderate confinement we have chosen.

## CHAPTER SEVEN

### CONCLUSION

The main aim of this thesis is to investigate theoretically the ground state structure of a parabolically confined quantum wire. Emphasis has also been set on exploring the effect of exchange-correlation energy, spin-orbit interaction and magnetic field to the energy dispersion.

We have studied the energy dispersion relations of the spin-split subbands for different cases such as different types of SO interaction, in the presence or absence of in-plane magnetic field and exchange-correlation energy. In this study we have taken account the contribution of the generally off-neglected cubic Dresselhaus terms. We have considered three different orientations of magnetic fields and we have seen that the energy subband structure depends on this orientation. We have investigated the energy subband structure for different types of SO interaction such as strong or weak SO interaction. The effect of exchange-correlation energy has also been searched. In this study the numerical calculations have been achieved high accuracy with a powerful method FEM. The electron energies have been calculated by FEM which is based on Galerkin procedure.

The energy dispersion has been obtained in the absence of magnetic field and SO interaction. The energy subbands has showed two-fold degeneracy. By applying an external magnetic field the time-reversal symmetry has been broken and the degeneracy has lifted but in some situations the degeneracy at the point  $k_x = 0$  has remained. It has been shown that the zero-k splitting in any subband not only arises from Zeeman splitting but also is not linear in the magnetic field. The zero k-splitting also depends on subband. We have investigated the structure of subbands for zero and different strength of magnetic field. When the strength of external magnetic field is increased, it leads to higher oscillations frequency so the gaps between subbands are extended and thus weakens the SO coupling. We have searched the effect of different types of SO interaction to the energy subband in the absence and presence of magnetic field. It has been observed that the SO interaction changes the k-splitting, leads to anticrossings between the different spin orientations within the same subband and couplings between differ-

ent subbands. We have shown that the interplay between the different magnetic field strengths and different SO coupling causes complex and intriguing energy spectrum. We have also searched the cubic Dresselhaus terms. It is shown that the contribution of the cubic Dresselhaus terms are efficient and it caused strong shifting in the energy subbands.

We have investigated the exchange-correlation effects on the ground state structure for the different strengths of SO interaction and in the absence or presence of an external in-plane magnetic field. The exchange-correlation energy has been calculated within the noncollinear local-spin density approximation in the density functional theory framework. We have obtained that exchange-correlation interaction contributes the existing magnetic field or acts as if an external magnetic field and produces the effect of magnetic field especially at low density values. It can be obviously seen in the energy subband structure. The most conspicuous properties appeared in the strong spin-orbit regimes where exchange-correlation potential induced splitting gives rise to the so-called anomalous plateaus. In the presence of both magnetic field and strong SO interaction local maxima has been appeared in the even subbands and it is important in the conductance. We have studied the effect of exchange-correlation energy for different density limits. In the high density limits we have had similar results as in the litterateur. But in the low density limits, there are some differences between the studies in the litterateur and ours. We have used different exchange-correlation energy functional from those existing works in which von Borth Hedin energy functional is used for calculating the effect of exchange-correlation potential. In this study, we have exploited Attaccalite prescription, which is commonly used recently, to calculate the exchange-correlation energy.

## REFERENCES

- Abonov, A. (2012). Spin resonance in a quantum wire: anomalous effects of an applied magnetic field. *Phys. Rev. B*, 85, (085311), 1-7.
- Alferov, I. Z. (2001). Nobel Lecture: The double heterostructure concept and its applications in physics, electronics, and technology. *Rev. Mod. Phys.*, 73, 767-782.
- Armiento, R. (2005). *The many-electron energy in density functional theory*. KTH School of Engineering Sciences:Ph.D.Thesis.
- Attaccalite, C., Moroni, S., Gori-Giorgi, P., & Bachalet, G. B. (2002). Correlation energy and spin polarization in the 2D electron gas. *Phys. Rev. Lett*, 88, (256601), 1-4.
- Attaccalite, C., Moroni, S., Gori-Giorgi, P., & Bachalet, G. B. (2003). Erratum:Correlation energy and spin polarization in the 2D electron gas [Phys. Rev. Lett. 88, 256601 (2002)]. *Phys. Rev. Lett*, 91, (109902), 1.
- Born, M., & Oppenheimer, J., R. (1927). On the quantum theory of molecules. *Ann. Der Phys.*, 84, (457), 1-24.
- Bychkov, Y. A., & Rashba, E. I. (1984). Oscillatory effects and the magnetic susceptibility of carriers in inversion layers. *J. Phys. C*, 17, 6039-6045.
- Canham, L. T. (1990). Silicon quantum wire array fabrication by electrochemical and chemical dissolution of wafers. *Appl. Phys. Lett.*, 57, (10), 1046-1048.
- Choi, H., Kakegawa, T., Akabori, M., Suzuhi, T., & Yamada, S. (2008). Spin-orbit interactions in high In-content InGaAs/InAlAs inverted heterojunctions for Rashba spintronics. *Physica E:Low-dimensional system and nanostructures*, 40, (8), 2823-2828.
- Citrin, D. S., & Chang, Y. C. (1989). Valance subband structures of  $GaAs/Al_xGa_{1-x}As$  quantum wires: The effect of splitt-off bands. *Phys. Rev. B*, 40, 5507-5514.
- de Picciotto, R., Storer, H. L., Pfeiffer, L. N., Baldwin, K. W., & West, K. W. (2001). Four-terminal resistance of a ballistic quantum wire. *Nature Physics*, 411, 51-54.

- Dietl, T. (1994). Dilute magnetic semiconductors. *Materials, properties and preparation (Handbook of semiconductor)*, 3B.
- Dietl, T. 2010. A ten-year perspective on dilute magnetic semiconductor and oxides. *Nat. Mat.*, 9, 965-974.
- Dresselhaus, G., (1955). Spin-orbit coupling effects in zinc blende structures. *Phys. Rev.*, 100, 580-586.
- Garcia, J. M., Gonzales, M. U., Silveria, J. P., Gonzales, Y., & Brianes, F. (2001). InAs/InP(0 0 1) quantum wire formation due to anisotropic stress relaxation: in situ stress measurements. *Journal of Crystal Growth*, 227-228, 975-979.
- Giuliani, G. F. & Vignale, V. (2005). *Quantum theory of the electron liquid*. New York:Cambridge University Press.
- Gonzales, L., Garcia, J. M., Garcia, R., Briones, F., Martinez-Postor, J., & Balles-teros, C. (2000). Influence of buffer-layer surface morphology on the self-organized growth of InAs on InP(001) nanostructures. *Appl. Phys. Lett.*, 76, (1104), 1-3.
- Griffiths, D., J., (1994). *Introduciton to quantum mechanics*. America:Prentice Hall.
- Gujarathi, S., Alam, K. M., & Pramanik, S. (2012). Magnetic-field-induced spin texture in a quantum wire with linear Dresselhaus spin-orbit coupling. *Phys. Rev. B*, 85, (045413), 1-14.
- Güneş, M. (2009). *Hidrostatik basınç altında düşük boyutlu yarı iletken sistemlerin elektronik ve optik özellikleri*. Cumhuriyet Üniversitesi:Ph.D.Theis.
- Harrison, P. (2005). *Quantum wells, wires and dots theoretical and computational physics of semiconductor nanostructures* (2nd edition) Wiley Interscience.
- Hartree, D., R., (1928). The calculation of atomic structures. *Proc. Cambridge Philos. Soc*, 24, (89), 113-143.
- Heinonen, O., Kinaret, J., M., & Johnson, M. D. (1999). Ensemble density-functional approach to charge-spin textures in inhomogeneous quantum Hall systems. *Phys. Rev. B*, 59, 8073-8083.

- Hohenberg, P., & Kohn, W. (1964). Inhomogeneous electron gas. *136*, (B864), 1912-1919.
- Hutton, D. V. (2004). *Fundamentals of Finite Element Analysis*. McGraw-Hill Science/Engineering/Math.
- Jalil, M. B. A., Tan, A. G., & Fujita, T. (2008). Spintronics in 2DEG systems. *AAPPS Bulletin*, *18*, (5), 9-20.
- Jones, R. O., & Gunnarsan, O. (1989). The density functional formalism, its applications and prospects. *Rev. Mod. Phys.*, *61*, 689-746.
- Kapon, E., Hwang, D. M., & Bhat, R. (1989). Stimulated emission in semiconductor quantum wire heterostructures. *Phys. Rev. Lett.*, *63*, 430-433.
- Knobbe, J., & Schapers, Th. (2005). Magnetosubbands of semiconductor quantum wires with Rashba spin-orbit coupling. *Phys. Rev. B*, *71*, (035311), 1-6.
- Kohn, W., & Sham, L. J. (1965). Self-consistent equations including exchange-correlation effects. *Phys. Rev.*, *140*, A1133-A1138.
- Kojimo, K., Mitsunga, K., & Kyuma, K. (1989). Calculation of two dimensional quantum-confined structures using the finite element method. *Appl. Phys. Lett.*, *55*, 882-884.
- Könemann, J., Haug, R. J., Maude, D. K., Fal'ko, V. I., & Altshuler, B. L. (2005). Spin-orbit coupling and anisotropy of spin splitting in quantum dots. *Phys. Rev. Lett.*, *94*, (226404), 1-4.
- Krich, J. J. & Halperin, B. I. (2007). Cubic Dresselhaus spin-orbit coupling in 2D electron quantum dots. *Phys. Rev. Lett.*, *98*, (226802), 1-4.
- Kübler, J., Höck, K.H., Sticht, J., & Williams, A. R. (1988). Density functional theory of non-collinear magnetism. *J. Phys. F:Met Phys.*, *18*, 469-483.
- Madelung, O. (1981). *Introduction to solid state theory*. Verlag:Springer
- Malet F., Marti P., & Baaranco M., Serra L., Lipparini E. (2007). Exchange-correlation effects on quantum wires with spin-orbit interactions under the influence of in-plane magnetic fields. *Phys. Rev. B* *76*, (115306), 1-12.



- Meijer, F. E. (2005). *Rashba spin-orbit interaction in mesoscopic systems*. Technische Universiteit Delft: Ph.D.Thesis.
- Miller, J. B., Zumbühl, D. M., Marcus, C. M., Lyanda-Geller, Y. B., Goldhaber-Gordon, D., Campman, K., & Gossard, A., C. (2003). Gate-controlled spin-orbit quantum interference effects in lateral transport. *Phys. Rev. Lett.*, *90*, (076807), 1-4.
- Nitta, J. (2004). Semiconductor spintronics. *Selected Papers*, *2*, (6), 1-6.
- Ogawa, M., Kunimasa, T., Ito, T., & Miyoshi, T. (1988). Finite-element analysis of quantum wires with arbitrary cross sections. *Journal of Applied Physics*, *84*, (3242), 1-8.
- Orellana, P. A., Dominguez-Adame, F., Gomez, I., & Ladrán de Guevara, M. L. (2003). Transport through a quantum wire with a side quantum-dot array. *Phys. Rev. B*, *67*, (085321), 1-5.
- Parr, R. G. & Yang, W. (1989). *Density-functional theory of atoms and molecules*. New York:Oxford University Press.
- Payne, M. C., Teter, M. P., Allan, D. C., Arios, T. A., & Joannopoulos, J. D. (1992). Iterative minimization techniques for ab initio total-energy calculations: molecular dynamics and conjugate gradients. *Rev. Mod. Phys.*, *64*, 1045-1097.
- Petroff, P. M., Gossard, A. C., Logan, R. A., & Wiegmann, W. (1982). Toward quantum well wires: Fabrication and optical properties. *Appl. Phys. Lett.*, *41*, (635), 1-4.
- Pfeiffer, L., West, K. W., Stormer, H. L., Eisenstein, J. P., Baldwin, K. W., Gershoni, D., & Spector, J. (1990). Formation of a high quality two-dimensional electron gas on cleaved GaAs. *Appl. Phys. Lett.*, *56*, (1697), 1-3.
- Pramanik, S., & Bandyopadhyay, S., Cahay, M. (2007). Energy dispersion relations of spin-split subbands in a quantum wire and electrostatic modulation of carrier spin polarization. *Phys. Rev. B*, *76*, (155325), 1-8.
- Pryor, C. (1991). Electronic structure and optical properties of serpentine superlattice quantum-wire arrays. *Phys. Rev. B*, *44*, 12912-12917.

- Quay, C. H. L., Hughes, T. L., Sulpizo, J. A., Pfeiffer, L. N., Baldwin, K. W., West, K. W., Goldhaber-Gordon, D., & de Picciotto, R. (2010). Observation of a one-dimensional spin-orbit gap in a quantum wire. *Nature Physics*, 6, 336-339.
- Rashba, E. I. (1960). Properties of semiconductors with an extremum loop. 1. Cyclotron and combinational resonance in a magnetic field perpendicular to the plane of the loop. *Sov. Phys. Solid State*, 2, (1109), 1224-1238.
- Sakurai, J. J. (1967). *Advanced quantum mechanics*. Addison:Wesley.
- Schliemann, J., Egues, J. C., & Loss, D. (2003). Non-ballistic spin field-effect transistor. *Phys. Rev. Lett.*, 90, (146801), 1-5.
- Searles, D. J., & von Nagy-Felsobuki, E.I. (1988). Numerical experiments in quantum physics: Finite element method. *Am. J. Phys.*, 56, 444-448.
- Serra, L., Sanchez, D., & Lopez, R. (2005). Rashba interaction in quantum wires with in-plane magnetic fields. *Phys. Rev. B*, 72, (235309), 1-6.
- Slater, J. C. (1930). Notes on Hartree's method. *Phys. Rev.*, 35, 210-211.
- Studer, M., Walser, M. P., Baer, S., Rusterholaz, H., Schön, S., Schuh, D., Wegscheider, W., Ensslin, K., & Salis, G. (2010). Role of linear and cubic terms for the drift-induced Dresselhaus spin-orbit splitting in a two-dimensional electron gas. *Phys. Rev. B*, 82, (235320), 1-6.
- Tongay, S. (2004). *Silicon and carbon based nanowires*. Bilkent University: Master Thesis
- Ungan, F. (2010). *Yoğun lazer alanı altında GaInAs/GaAs kuantum kuyularındaki donör safsızlık atomlarının bağlanma enerjileri*. Cumhuriyet Üniversitesi:Ph.D. Thesis.
- von Borth, H., & Hedin, L. (1972). A local exchange-correlation potential for the spin polarized case. *J. Phys. C: Solid State Phys.*, 5, 1629-1642.
- Wagner, R. (2009). *G-factor, effective mass and spin susceptibility of a 2-dimensional electron gas*. University of Basel:Master Thesis.
- Wolf, J. P. (2003). *The scaled boundary finite element method* (1st ed). England:Wiley.

- Wrinkler, R. (2003). *Spin-orbit coupling effects in two dimensional electron and hole systems*. New York:Springer.
- Wu, M. W., Jiang, J., & Weng, M. Q. (2010). Spin dynamics in semiconductors. *Phys. Reports*, 493, 2-4.
- Yamauchi, T., Takahasi, Y. T., & Arakawa, Y. (1991). Tight binding analysis for quantum wire lasers and quantum wire infrared detectors. *IEEE J. Quantum Electron*, 27, 1817-1823.
- Yeşilgül, Ü. (2010). *GaInAs/GaAs kuyularında ekzitonik yapının yoğun lazer alanı yaklaşımı altındaki davranışı*. Cumhuriyet Üniversitesi:Ph.D. Thesis.
- Yi, J. C., & Dagli, N. (1995). Finite element analysis of valance band structure and optical properties of quantum-wire arrays on vicinal substrates. *IEEE J. Quantum Electron*, 31, 208 - 218.
- Zhang., S., Liang, R., Zhang, E., Zhang, L., & Liu, Y. (2006). Magnetosubbands of semiconductor quantum wires with Rashba and Dresselhaus spin-orbit coupling. *Phys. Rev. B*, 73, (155316), 1-7.
- Zhang, T., Zhao, W., & Liu, X. (2009). Energy dispersion of the electrosubbands in parabolic confinement quantum wires: interplay of Rashba, Dresselhaus, lateral spin-orbit interaction and the Zeeman effect. *J. Physics.:Condens. Matter*, 21, (335501), 1-9.
- Zienkiewicz, O. C., Taylor, R. L., & Zhu, J. Z. (2005). *The Finite Element Method: Its Basis and Fundamentals* (5th ed). Spain:Planta Tree.
- Zutic, I., Fabian, J., & Sarma Das, S. (2004). Spintronics:Fundamentals and applications. *Rev. Mod. Phys.*, 76, 232-410.